

Depth-extrapolation of field-scale soil moisture time series derived with cosmic-ray neutron sensing using the SMAR model

Daniel Rasche¹, Theresa Blume¹, and Andreas Güntner^{1,2}

¹GFZ German Research Centre for Geosciences, Section Hydrology, 14473, Potsdam, Germany

²University of Potsdam, Institute of Environmental Sciences and Geography, 14476, Potsdam, Germany

Correspondence: Daniel Rasche (daniel.rasche@gfz-potsdam.de)

Abstract. ~~Soil~~ Ground-based soil moisture measurements at the field-scale are highly beneficial for different hydrological applications including the validation of space-borne soil moisture products, landscape water budgeting or multi-criteria calibration of rainfall-runoff models from field to catchment scale. ~~Many of these applications require information on soil water dynamics in deeper soil layers.~~ Cosmic-ray neutron sensing (CRNS) allows for non-invasive monitoring of field-scale soil moisture across several hectares around the instrument but only for the first few tens of centimeters of the soil. Many of these applications require information on soil water dynamics in deeper soil layers. Simple depth-extrapolation approaches often used in remote sensing applications may be used to estimate soil moisture in deeper layers based on the near-surface soil moisture information. However, most approaches require a site-specific calibration using depth-profiles of in-situ soil moisture data, which are often not available. The ~~physically-based~~ soil moisture analytical relationship SMAR is usually also calibrated to sensor data, but due to the physical meaning of each model parameter, it could be applied without calibration if all its parameters were known. However, in particular its water loss parameter is difficult to estimate. In this paper, we introduce and test a simple modification of the SMAR model to estimate the water loss in the second layer based on soil physical parameters and the surface soil moisture time series. We apply the model with and without calibration at a forest site with sandy soils ~~with and without calibration~~. Comparing the model results ~~against with~~ in-situ reference measurements down to depths of 450 cm shows that the SMAR models both with and without modification as well as the calibrated exponential filter approach do not capture the observed soil moisture dynamics well. ~~The~~ While, on average, the latter performs best over different tested scenarios, the performance of the SMAR models nevertheless meets a previously used benchmark RMSE of $\leq 0.06 \text{ cm}^3 \text{ cm}^{-3}$ in both, ~~calibrated and uncalibrated scenarios. Only with effective parameters in a non-physical range, a better model performance could be achieved.~~ the calibrated original and uncalibrated modified version. Different transfer functions to derive surface soil moisture from CRNS do not translate into markedly different results of the depth-extrapolated soil moisture time series simulated with SMAR. ~~However, a more accurate estimation of the sensitive measurement depth of the CRNS improved the soil moisture estimates in the second layer.~~ Despite the fact that the soil moisture dynamics are not well represented at our study site using ~~physically reasonable parameters, the~~ the depth-extrapolation approaches, our modified SMAR model may provide valuable first estimates of soil moisture in a deeper soil layer derived from surface measurements based on stationary and roving CRNS as well as remote sensing products where in-situ data for calibration are not available.

1 Introduction

Soil moisture is a key parameter in the hydrological cycle (e.g., Vereecken et al., 2008, 2014; Seneviratne et al., 2010). It controls several aspects of the environment such as soil infiltration, runoff dynamics, plant growth and biomass production which in turn influence evapotranspiration as well as the climatic conditions on varying spatio-temporal scales (see reviews
30 by e.g., Daly and Porporato, 2005; Vereecken et al., 2008; Seneviratne et al., 2010; Wang et al., 2018). Thus, information on soil water dynamics at the field-scale have great importance for various larger-scale hydrological applications ranging from landscape water budgeting to multi-criteria calibration approaches in rainfall-runoff modeling. However, due to the high spatio-temporal variability of soil water content (Famiglietti et al., 2008; Vereecken et al., 2014) which is highest in surface soil layers (Babaeian et al., 2019), measuring field-scale soil moisture and its dynamics proves difficult based on invasive point-scale soil
35 moisture measurement methods as for example reviewed in Vereecken et al. (2014) and Babaeian et al. (2019). For instance, the installation of electromagnetic point sensors measuring at high temporal resolution would require a very large number of sensors to obtain a representative field-scale average (Babaeian et al., 2019). Additionally, sensor networks are not always feasible as agricultural management practices hamper a permanent installation of point sensors (Stevanato et al., 2019). As a consequence, extensive point sensor networks which allow for the estimation of field-scale soil moisture are often restricted
40 to a rather small number of research related monitoring sites such as the Terrestrial Environmental Observatories (TERENO, www.tereno.net) in Germany (e.g., Zacharias et al., 2011; Bogena et al., 2018; Kiese et al., 2018; Heinrich et al., 2018) [or the International Soil Moisture Monitoring Network \(ISMN, Dorigo et al., 2021\) covering sites around the globe.](#)

Kodama et al. (1979), Kodama et al. (1985) and Dorman (2004) suggested the potential of naturally occurring secondary neutrons produced by high-energy cosmic rays for estimating soil and snow water. About a decade ago Zreda et al. (2008);
45 Desilets et al. (2010), introduced a methodological framework for soil moisture estimation using cosmic-ray neutrons. The cosmic-ray neutron sensing (CRNS) approach is a non-invasive geophysical method for estimating representative field-scale soil moisture (Schrön et al., 2018b) based on the measurement of cosmic-ray neutrons which are inversely related to the amount of hydrogen in the vicinity of the neutron detector. As soil water is the largest pool of hydrogen in the footprint of the neutron detector in most terrestrial environments, CRNS allows for the measurement of integrated soil moisture of several hectares
50 around the instrument and the first decimetres of the soil (e.g., Zreda et al., 2008; Desilets et al., 2010; Köhli et al., 2015; Schrön et al., 2017).

Estimating soil moisture using CRNS has a high potential for various hydrological applications, which require soil moisture observations at the field-scale. Several studies demonstrate the potential of CRNS-derived soil moisture estimates for example for a comparison with satellite derived soil moisture products, their validation and the improved calibration of environmental
55 models (e.g., Holgate et al., 2016; Montzka et al., 2017; Iwema et al., 2017; Duygu and Akyürek, 2019; Dimitrova-Petrova et al., 2020). Besides stationary CRNS probes for the retrieval of field scale soil moisture time series, roving CRNS-devices have been successfully used, mapping CRNS-derived surface soil moisture in even larger areas with instruments mounted on vehicles (e.g., McJannet et al., 2017; Schrön et al., 2018a; Vather et al., 2019) and (Fersch et al., 2018) illustrate potential synergies between CRNS, airborne radar and in-situ point sensor networks for soil moisture estimation across spatial scales. Due to the

60 sensitivity of CRNS to any hydrogen in the measurement footprint, snow monitoring (e.g., Schattan et al., 2017, 2019; Gugerli et al., 2019), irrigation management (e.g., Li et al., 2019a) as well as biomass estimation (e.g., Baroni and Oswald, 2015; Tian et al., 2016; Jakobi et al., 2018; Vather et al., 2020) pose further fields of application and are reviewed in Andreasen et al. (2017).

Although the large areal footprint of the CRNS-instrument allows estimating field-scale integral soil moisture, the CRNS-
65 derived time series lack soil moisture information from greater depths. However, soil moisture at these greater depths becomes highly relevant as soon as the rooting depth of crops or forest extends past the first decimeters. The maximum rooting depth and hence, root zone extent as well as root density along the soil profile varies with vegetation type and biome (e.g., Canadell et al., 1996; Jackson et al., 1996). According to Jackson et al. (1996), on global average across all biomes, the 75 percent of plant roots occur in the first 40 centimetres of the soil, which would be largely covered by the CRNS. However, the global
70 average maximum rooting depth, and thus, root zone depth is about 4.6 m (Canadell et al., 1996) where the rooting depth also depends on prevailing soil hydrological conditions (Fan et al., 2017). Even grassy vegetation and crops can have rooting depths of more than 200 cm (Canadell et al., 1996), thus exceeding the measurement depth of CRNS. Deep roots play a significant role for the water supply of plant ecosystems especially during dry conditions (Canadell et al., 1996) i.e. through hydraulic redistribution (see e.g., Neumann and Cardon, 2012) or increased root water uptake from deeper soil layers under drought con-
75 ditions (Maysonnave et al., 2022). Furthermore, plant species influence infiltration and vertical soil moisture patterns through species dependent root distributions (e.g. Jost et al., 2012) and horizontal soil moisture patterns through species dependent evapotranspiration and interception rates (e.g. Schume et al., 2003). Hence, field-scale soil water information from the deeper vadose zone overcoming these smaller scale heterogeneities can be important for the quantification of water storage variations, potential influences on vegetation dynamics, matter fluxes and the characterization of the local hydrological cycle.

80 Given the importance of soil moisture in the deeper root zone, extending CRNS-measurements to greater depths is of high importance for broadening the applicability of CRNS for soil water estimations (Peterson et al., 2016). Numerous studies extrapolate surface soil moisture time series to greater depths using different empirical approaches (e.g., Zhang et al., 2017; Li and Zhang, 2021) including regression analyses, machine learning techniques or other approaches such as the [exponential filter](#)/soil water index (SWI) (Wagner et al., 1999; Albergel et al., 2008). Few studies address the depth-extrapolation of field-
85 scale CRNS-derived soil moisture time series (e.g., Peterson et al., 2016; Zhu et al., 2017; Nguyen et al., 2019; Franz et al., 2020) to the shallow root zone (approx. 100 cm) by applying and comparing extrapolation approaches with the SWI being the most commonly used approach (e.g., Peterson et al., 2016; Dimitrova-Petrova et al., 2020; Franz et al., 2020). All these approaches require reference soil moisture information in the depth of interest to either build an empirical model or calibrate the depth-extrapolated soil moisture time series. This information may not always be available in sufficient quantity and quality.
90 In contrast, the physically-based soil moisture analytical relationship (SMAR) (Manfreda et al., 2014), applied and modified in recent studies (e.g., Faridani et al., 2017; Baldwin et al., 2017, 2019; Gheybi et al., 2019; Zhuang et al., 2020; Farokhi et al., 2021), allows for the extrapolation of daily surface soil moisture information to a second, lower soil layer by solely relying on soil physical information and a water loss term. This method does not require calibration if the environmental parameters are known.

95 Against this background, we investigate the potential to depth-extrapolate ~~hourly and~~ daily surface soil moisture time series without calibration and thus without the need for reference soil moisture information in the depth of interest by applying the SMAR algorithm at a highly ~~equipped-instrumented~~ study site in the TERENO-NE observatory located in the lowlands of north-eastern Germany. While soil physical parameters may be determined from soil ~~analyses~~samples or directly in-situ, the water loss parameter describing the water loss per unit time from the second soil layer is more difficult to estimate. Therefore, 100 we propose a simple modification of the SMAR algorithm to estimate the water loss term from soil physical characteristics and from the surface soil moisture time series~~derived from CRNS~~. We first compare the standard SMAR that uses a constant, calibrated water loss term (calibrated against in-situ reference sensors) with the modified, uncalibrated SMAR that uses the estimated ~~water term loss~~ water-loss term for different depths of the second soil layer down to 450 cm~~depth~~. ~~Secondly, we calibrate all soil parameters in the original and modified version.~~ For comparison with the two versions of the SMAR 105 model~~in order to assess its best possible performance at the study site for the given in-situ reference data. In addition, we apply different neutron-to-soil moisture transfer functions available to derive the~~, we also calibrate the exponential filter approach (Wagner et al., 1999; Albergel et al., 2008) for the study site.

Different approaches exist to derive soil moisture from observed neutron signals. The standard approach after Desilets et al. (2010) is commonly used to derive soil moisture from CRNS but has been found insufficient especially at observation sites with low 110 soil moisture contents. New approaches include the interdependence of the relationship between neutrons and soil moisture (Köhli et al., 2021) and report an improved estimation of surface soil moisture ~~time series. This is done to assess which transfer function performs best with CRNS.~~

The three depth-extrapolation approaches (SMAR, modified SMAR and exponential filter) are therefore applied using different surface soil moisture time series, including single point-scale in-situ sensor profiles, averages of the entire in-situ 115 sensor network and CRNS-derived soil moisture from different neutron-to-soil moisture transfer functions in order to investigate the performance of the different approaches and if a better CRNS-derived surface soil moisture time series translates into better estimates of the depth-extrapolated soil moisture. ~~Lastly, we test the influence of the choice of the depth of first soil layer, i.e. the sensitive measurement depth of CRNS, on the goodness-of-fit of the depth-extrapolated to soil moisture estimates.~~

2 Material and methods

120 2.1 Study site

The study site is located in the TERENO-NE observatory (Heinrich et al., 2018) in the young Pleistocene landscape of north-eastern Germany (Fig. 1). The site hosts the CRNS sensor „Serrahn“ (Bogena et al., 2022). The site has a mean annual temperature of 8.8°C and mean annual precipitation of 591 mm per year, measured at the long-term weather station in Waren (in a distance of approximately 35 km) operated by the German Weather Service (station ID: 5349, period 1981–2010) (DWD 125 - German Weather Service, 2020a, b). It is situated on the southern ascent of a glacial terminal moraine formed during the Pomeranian phase of the Weichselian glaciation in the Pleistocene (Börner, 2015). The dominating soil types in the vicinity of the sensor are Cambisols formed on aeolian sands with depths down to 450 cm deposited during the Holocene (Rasche et al.,

2023). Continuing downwards, these are followed by deposited glacial till of the terminal moraine, glacio-fluvial sediments and glacial tills originating from earlier glaciations with the latter forming the aquitard the upper groundwater aquifer with water level depths ranging between 13 and 14 m below the surface (Rasche et al., 2023). A mixed forest dominated by European beech (*Fagus sylvatica*) and Scots pine (*Pinus sylvestris*) is the dominant landcover type. A clearing covered by grassy vegetation can be found nearby.

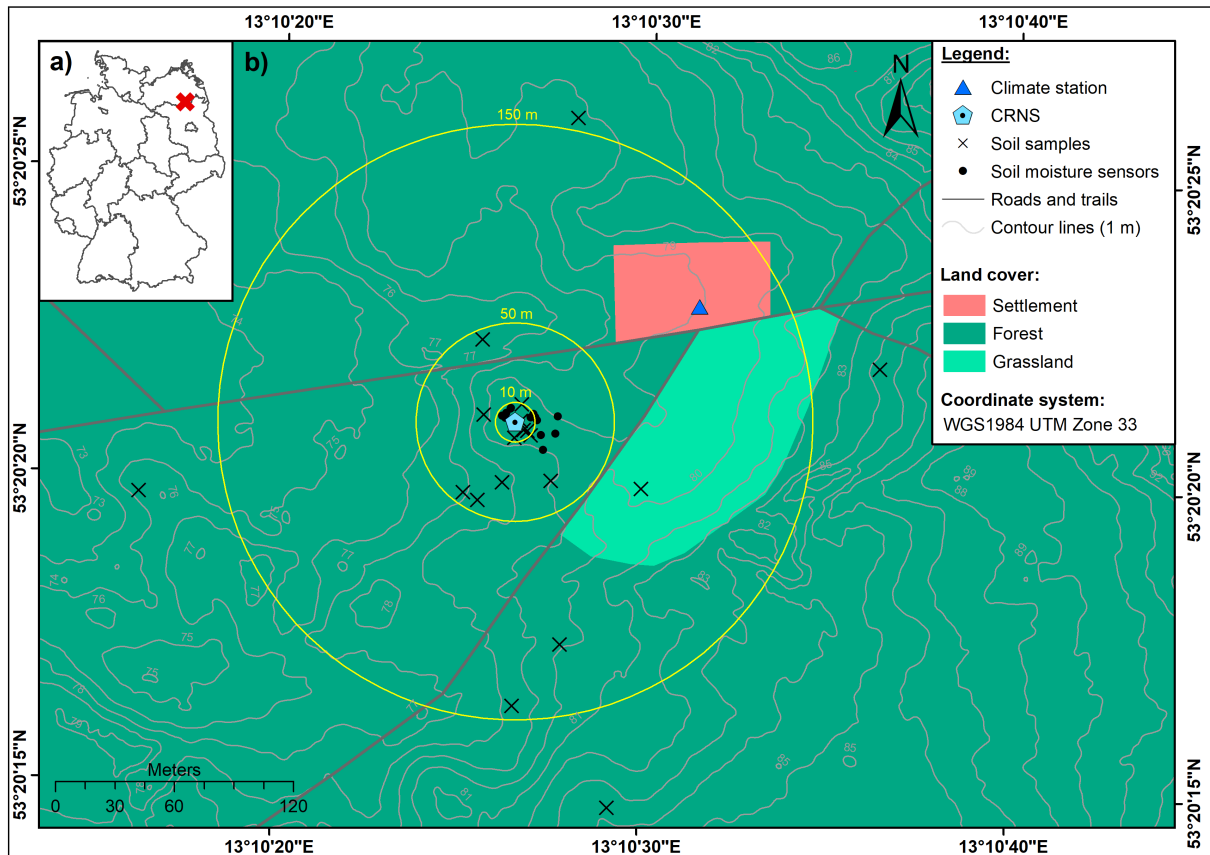


Figure 1. Location of the study area within Germany (a) and location of the CRNS observation site „Serrahn“ (b) (digital elevation model: LAIV-MV - State Agency for Interior Administration Mecklenburg-Western Pomerania (2011), land cover: BKG - German Federal Agency for Cartography and Geodesy (2018)).

In order to calibrate the CRNS sensor, soil samples were taken at different distances around the instrument in February 2019 as shown in Fig. 1. Soil samples were taken in 5 cm depth increments from 0–35 cm using a split tube sampler containing sampling rings in order to derive soil moisture, soil physical characteristics, average grain size distributions, soil organic matter and lattice water from laboratory analyses as shown in Tab. 1. Soil moisture and soil bulk density were determined from oven-drying at 105°C for 12 h and gravimetric analyses of all individual soil samples. Subsequent loss-on-ignition analyses at 550

and 1000°C with a duration of 24 h were used to determine the amount of soil organic matter and lattice water from bulk samples per depth assuming that no inorganic carbon is present in the acidic aeolian sands. Soil porosity was estimated based on the material density of quartz (2.65 g cm^{-3}) and corrected for the amount of soil organic matter based on the density of cellulose (1.5 g cm^{-3}).

In addition to the stationary CRNS instrument, the study site is equipped with a groundwater observation well, a weather station and a network of in-situ point-scale soil moisture sensor profiles (type SMT100; Truebner GmbH, Germany). A total of 59 in-situ soil moisture sensors is deployed in depths down to 450 cm depth with 12 sensors in 10 cm, 6 sensors in 20 cm, 8 sensors in 30 cm, 8 sensors in 50 cm, 6 sensors in 70 cm, 4 sensors in 130 cm, 7 sensors in 200 cm, 4 sensors in 300 cm as well as 450 cm. The sensors are located in distances up to 22 m from the CRNS instrument and continuously monitor the volumetric soil moisture content based on the manufacturer's calibration function.

Table 1. Soil physical characteristics at the CRNS site Serrahn obtained from laboratory analyses of soil samples (Rasche et al., 2023, modified). Below the maximum sampling depth of 35 cm and down to the maximum depth of the aeolian sand deposits, the soil physical are assumed to have the same soil physical parameters as the layer between 30 and 35 cm. The soil moisture content at field capacity and wilting point were taken from tabulated values in Sponagel et al. (2005) according to the respective soil grain size class (medium-fine sand) and the soil bulk density of the individual layers.

Depth [cm]	Grain size fractions [weight-%]					Bulk density [g cm^{-3}]	Porosity [-]	Organic matter [g g^{-1}]	Lattice water [g g^{-1}]	Field capacity [$\text{cm}^3 \text{ cm}^{-3}$]	Wilting point [$\text{cm}^3 \text{ cm}^{-3}$]
	> 2 mm	2 - 0.63 mm	0.63 - 0.2 mm	0.2 - 0.063 mm	< 0.063 mm						
0-5	2.7	19.7	42.2	33.7	2.1	0.24	0.91	0.32	0.003	0.16	0.06
5-10	1.1	8.7	43.5	45.7	2.4	0.77	0.70	0.10	0.002	0.16	0.06
10-15	0.7	7.2	41.5	47.9	2.8	1.25	0.52	0.05	0.002	0.16	0.06
15-20	1.2	7.8	38.7	44.3	2.2	1.43	0.45	0.02	0.002	0.14	0.05
20-25	1.7	7.7	42.2	46.5	2.2	1.55	0.41	0.02	0.002	0.14	0.05
25-30	1.7	8.5	43.5	45.4	1.2	1.59	0.40	0.01	0.002	0.12	0.04
30-35	1.1	8.0	42.8	46.8	1.5	1.63	0.38	0.01	0.002	0.12	0.04
35-450	1.1	8.0	42.8	46.8	1.5	1.63	0.38	0.01	0.002	0.12	0.04

2.2 Field-scale surface soil moisture derived with CRNS

Secondary neutrons are produced by primary cosmic-rays interacting with matter in the atmosphere and in the ground. Depending on their energy level, secondary neutrons may be classified as fast (0.1-10 MeV), epithermal (> 0.25-100 keV) and thermal neutrons (< 0.25 eV) (e.g., Köhli et al., 2015; Weimar et al., 2020). Cosmic-ray neutron sensing for soil moisture estimation relies on the amount of neutrons in the epithermal energy range produced by nuclear evaporation in the atmosphere and ground (Köhli et al., 2015). Epithermal neutrons are sensitive to elastic scattering by collision with hydrogen and are further moderated to thermal neutrons (< 0.25 eV). Thus, the amount of epithermal neutrons detected by the instrument is inversely correlated with the amount of hydrogen in the sensitive measurement footprint of the sensor.

Epithermal neutron counts detected by the instrument are influenced by atmospheric pressure, the amount of primary high-energy cosmic-ray neutrons entering the earth's atmosphere from space (Zreda et al., 2012) as well as variations of absolute air humidity (Rosolem et al., 2013) and need to be corrected for these influencing factors before soil moisture information can be derived. In this study, we use the correction procedure for air pressure and incoming primary cosmic-ray flux presented in
160 Zreda et al. (2012). The correction factor for the shielding effect of the atmosphere can be calculated from local air pressure measurements where the attenuation length L is set to 135.9 g cm^{-2} for the study area (Heidbüchel et al., 2016). The correction factor for the incoming high-energy primary neutron flux was obtained from hourly pressure and efficiency corrected primary neutron intensities (cps) of the Jungfraujoch neutron monitor (JUNG, www.nmdb.eu). Furthermore, the neutron data was corrected for the influence of absolute air humidity introduced by Rosolem et al. (2013). The absolute humidity is calculated
165 from relative humidity and temperature observations of the weather station at the observation site according to Rosolem et al. (2013). For all correction approaches, the time series averages of air pressure, incoming radiation and air humidity are used as the required reference values. Finally, a 25 h moving average filter is applied to the corrected neutron time series to reduce noise and uncertainty in the data (e.g., Schrön et al., 2018b).

$$\theta_{\text{Standard}} = \left(\left(\tilde{a}_0 \frac{1 - \frac{N_{\text{pih}}}{N_{\text{max}}}}{\tilde{a}_1 - \frac{N_{\text{pih}}}{N_{\text{max}}}} \right) \times \frac{\rho_{\text{soil}}}{\rho_{\text{water}}} \right) - (\theta_{\text{SOM}} + \theta_{\text{LW}}), \quad (1)$$

170 where

$$\tilde{a}_0 = -a_2, \quad (2)$$

$$\tilde{a}_1 = \frac{a_1 a_2}{a_0 + a_1 a_2}, \quad (3)$$

$$N_{\text{max}} = N_0 \cdot \frac{a_0 + a_1 a_2}{a_2}. \quad (4)$$

Desilets et al. (2010) introduced a transfer function to convert neutron counts into soil moisture by calibration against
175 reference measurements. Although other approaches exist (e.g., Franz et al., 2013; Köhli et al., 2021), the Desilet's equation became the methodological standard and can be rewritten as eq. (1) – (4) (Köhli et al., 2021) with $a_0 = 0.0808$, $a_1 = 0.372$, $a_2 = 0.115$ and N_0 being a local calibration parameter describing the neutron intensity above dry soil (Desilets et al., 2010). As observed epithermal neutron intensities are sensitive to any hydrogen present in the measurement footprint, the water equivalent of soil organic matter θ_{SOM} and the amount of lattice water θ_{LW} in $\text{cm}^3 \text{ cm}^{-3}$ need to be subtracted. Additionally, ρ_{soil}
180 describes the average soil bulk density in the measurement footprint (g cm^{-3}) and ρ_{water} the density of water assumed to be 1 g cm^{-3} . In this neutron-to-soil moisture transfer function the neutron intensity corrected for variations in air pressure, incoming

primary neutron flux and absolute humidity N_{pih} is used. However, the more recent study by Köhli et al. (2021) suggests that the influence of absolute air humidity and soil moisture on the observed epithermal neutron signal are interdependent, i.e. the shape of the neutron-soil moisture relationship changes with absolute humidity. The universal transport solution (UTS), eq. (5) – eq. (6), (Köhli et al., 2021) accounts for the changing relationship between neutrons and soil moisture under different conditions of absolute humidity h in g cm^{-3} .

$$N_{pi} = N_D \cdot \left(\frac{p_1 + p_2 \theta_{\text{total}}}{p_1 + \theta_{\text{total}}} \cdot (p_3 + p_4 h + p_5 h^2) + e^{-p_6 \theta_{\text{total}}} (p_7 + p_8 h) \right), \quad (5)$$

where

$$\theta_{\text{total}} = (\theta_{\text{UTS}} + \theta_{\text{SOM}} + \theta_{\text{LW}}) \cdot \frac{1.43 \text{ g cm}^{-3}}{\rho_{\text{soil}}} \quad (6)$$

The UTS is designed to describe the neutron intensity response caused by changes in total soil water content and absolute air humidity and therefore, the predicted neutron intensity represents the intensity corrected for variations in atmospheric pressure and incoming primary neutron flux N_{pi} . Soil moisture can be derived from the UTS using numerical inversion or a look-up table approach which is used in this study. In the look-up table approach, soil moisture values in the range from 0.0001 to 0.5 $\text{cm}^3 \text{cm}^{-3}$ in steps of 0.0001 $\text{cm}^3 \text{cm}^{-3}$ are used to predict the neutron intensity using the UTS for each time step. For each time step, the soil moisture value producing the smallest absolute difference between the observed and predicted neutron intensity is then assigned as the CRNS-derived soil moisture value. Analogously to the standard transfer function, the UTS needs to be calibrated locally. The calibration parameter N_D may be interpreted as the average neutron intensity of the local neutron detector under the boundary conditions defined in the neutron transport simulations which were used to subsequently derive the UTS. θ_{total} describes the total water content comprising the sum of all below-ground hydrogen pools, namely the soil moisture content θ_{UTS} , θ_{SM} and θ_{LW} which is then scaled by ratio of the soil bulk used in the neutron transport simulations to derive the UTS (1.43 g cm^{-3}) and the local soil bulk density at the study site ρ_{soil} (Köhli et al., 2021). Different sets of shape-giving parameters $p_1 - p_{10}$ are available for the UTS in Köhli et al. (2021) and originate from the different neutron transport models used and whether a simple energy window threshold (thl) was used (parameter sets: URANOS thl, MCNP thl) to evaluate the neutron transport simulations or a more complex detector response function was applied (parameter sets: URANOS drf, MCNP drf). The latter mimics the response of a real neutron detector and is therefore expected to provide more accurate results. In the scope of this study, we investigate which of the two transfer functions and which parameter set of the UTS performs best in estimating surface soil moisture.

The CRNS footprint diameter as well as the integration depth decrease with i.e. increasing soil water content. The radius ranges between 130 and 240 m and the integration depth ranges between 15 and 83 cm during wet and dry conditions, respectively (Köhli et al., 2015). In addition, further factors may influence the footprint dimensions such as open water or topography (e.g., Köhli et al., 2015; Schattan et al., 2019; Mares et al., 2020). Consequently, reference measurements need to be depth-distance weighted according to the sensitivity of the CRNS instrument in order to match field observations of reference

measurements when calibrating the two different transfer functions and derive soil moisture information from observed neutron intensities. In this study, we adapt the weighting procedure proposed by Schrön et al. (2017) which takes the total water content, average bulk density, absolute air humidity and vegetation height (set to 20 m) into account. Reference soil moisture information from the soil sampling campaign in February 2019 was weighted accordingly and used for calibrating both transfer functions. N_0 and N_D were iteratively calibrated. For N_0 , the value producing the smallest RMSE between soil moisture from soil samples and the one predicted with eq. (1)–(4) was chosen. For N_D , soil moisture information derived from soil samples for the hours of the sampling campaign were used to predict neutron intensities with eq. (5)–(6). The N_D producing the smallest RMSE between predicted and observed neutron intensities was chosen. In a second step, the CRNS-derived soil moisture time series are compared to an analogously weighted average of all available in-situ soil moisture sensors in 10, 20 and 30 cm depth. In order to assess the impact of weighting procedure, the calibration is repeated using the arithmetic soil moisture average from soil samples and comparing the CRNS-derived soil moisture time series to the arithmetic average soil moisture time series from in-situ sensors.

2.3 Depth-extrapolation of surface soil moisture time series ~~from CRNS~~

2.3.1 Modification of the SMAR model

To estimate depth-extrapolated soil moisture time series for a second, deeper soil layer from ~~CRNS-derived~~ surface soil moisture time series, the SMAR model is used. Introduced by Manfreda et al. (2014), it allows for the physically-based estimation of soil moisture in an adjacent second, lower soil layer from soil moisture information in a first, upper soil layer. SMAR is based on the relative saturation in the first and second layer s_1 (-) and s_2 (-), respectively, the relative saturation at field capacity sc_1 (-) and wilting point sw_2 (-). In order to transform values from $\text{cm}^3 \text{cm}^{-3}$ to relative saturation, the respective variables are divided by the porosity of the individual layer n_1 ($\text{cm}^3 \text{cm}^{-3}$) and n_2 ($\text{cm}^3 \text{cm}^{-3}$). After applying the SMAR model, the resulting relative saturation time series of the second layer s_2 (-) is transformed back to volumetric soil moisture in $\text{cm}^3 \text{cm}^{-3}$ by multiplication with n_2 ($\text{cm}^3 \text{cm}^{-3}$) and resulting in the depth-extrapolated soil moisture time series $\theta_{\text{Layer } 2}$. Soil moisture in layer 2 at time t is calculated with

$$s_2(t_i) = s_{w2} + (s_2(t_{i-1}) - s_{w2}) \cdot e^{-a \cdot (t_i - t_{i-1})} + (1 - s_{w2}) \cdot b \cdot y(t_i) \cdot (t_i - t_{i-1}), \quad (7)$$

where a and b depend on the vertical extent of the first layer (Zr_1 in mm) which begins at the soil surface, and the vertical extent of the second layer (Zr_2 in mm). Zr_2 is the difference between the maximum depth of the second soil layer and Zr_1 . The water loss term V_2 (mm t^{-1}) comprises the bulk water losses from the second layer due to percolation and evapotranspiration per unit time:

$$a = \frac{V_2}{(1 - s_{w2}) \cdot n_2 \cdot Zr_2}, \quad (8)$$

$$b = \frac{n_1 \cdot Zr_1}{(1 - s_{w2}) \cdot n_2 \cdot Zr_2}, \quad (9)$$

The fraction of saturation of the first layer that instantaneously infiltrates into the second layer $y(t_i)$ (-) is described as (e.g.,
 245 Manfreda et al., 2014; Patil and Ramsankaran, 2018):

$$y(t_i) = \begin{cases} (s_1(t_i) - s_{c1}), & s_1(t_i) \geq s_{c1} \\ 0, & s_1(t_i) < s_{c1}. \end{cases} \quad (10)$$

The SMAR model can be applied using known soil physical and environmental variables. However, although the soil physical
 parameters may be estimated through pedotransferfunctions, using tabulated values or global soil databases (e.g. SoilGrids 2.0
 (Poggio et al., 2021)), the bulk water loss from the second layer V_2 is more difficult to estimate. This hampers the use of
 250 SMAR without calibration against reference soil moisture information in the depth of interest, i.e., in the deeper soil layer.
 To overcome this issue we modified and extended the SMAR model (SMAR_{mod}) in order to estimate the V_2 based on simple
 soil physical, environmental variables and the surface soil moisture time series. A modification of the SMAR model with an
 extended definition of the water loss term V_2 has been suggested by Faridani et al. (2017) leading to an improved performance
 compared to the original SMAR model. As any modification makes the SMAR model more complex and potentially less easy
 255 to apply, our aim was to keep the added complexity to the model low by only including 3 additional parameters. These are the
 relative saturation at field capacity in the second layer s_{c2} (-) and the cumulative root fraction to the maximum depth of the
 first and second layer R_1 (-) and R_2 (-), respectively. The water loss term is then defined as the sum of evapotranspiration ET_2
 (mm t^{-1}) and percolation P_2 (mm t^{-1}) from the second layer.

$$V_2 = ET_2 + P_2, \quad (11)$$

260 We adapt the suggestion of Manfreda et al. (2014) to make use of existing (surface) soil moisture time series to gain in-
 formation about water loss from the soil by evapotranspiration at a study site. Here, we estimate the individual amount of
 evapotranspiration from the deeper layer ET_2 for each time step based on the difference between the current and past value of
 relative saturation of the first layer, by scaling the value to the dimension (i.e. extent) of second layer and by considering the
 difference in cumulative root fraction between both layers, assuming that root water uptake for ET is larger in the layer with
 265 more roots eq. (13). The required root fraction R (-) for maximum depth d (cm) of the first and second layer are derived from
 the empirical equation (eq. 12) for forest biomes presented in Jackson et al. (1996):

$$R = 1 - 0.970^d \quad (12)$$

Using eq. 13, ET_2 can only be estimated from the change in relative saturation in the first layer when 1) the relative saturation of the first layer s_1 decreases, 2) no infiltration into the second layer occurs and 3) the relative saturation of the second layer exceeds the relative saturation at wilting point. This means that both, surface evaporation and transpiration losses are scaled from the first layer to the second layer. Although surface evaporation is hardly relevant for the second layer due to its missing connection with the surface, this is a reasonable yet simplified approach because surface evaporation is a comparatively small component of total evapotranspiration in forests, with transpiration dominating ET (e.g., Li et al., 2019b; Paul-Limoges et al., 2020).

$$ET_2(t_i) = \begin{cases} (s_1(t_i - 1) - s_1(t_i)) \cdot n_1 \cdot Z_{r1} \cdot \frac{Z_{r2}}{Z_{r1}} \cdot \frac{(R_2 - R_1)}{R_1}, & s_1(t_i - 1) \geq s_1(t_i); y(t_i) > 0; s_2(t_i - 1) \leq s_{w2} \\ 0, & otherwise. \end{cases} \quad (13)$$

The amount of percolation P_2 from the second layer is estimated in analogy to the infiltration into this layer as an instantaneous water loss when the relative saturation exceeds field capacity sc_2 (eq. 14).

$$P_2(t_i) = \begin{cases} (s_2(t_i - 1) - sc_2), & s_2(t_i - 1) \geq sc_2 \\ 0, & s_2(t_i - 1) < sc_2. \end{cases} \quad (14)$$

2.3.2 Application of Comparison with the SMAR model exponential filter method

To evaluate the performance of the original SMAR and the modified version $SMAR_{modified}$, we also compared it to the exponential filter approach (soil water index SWI, Wagner et al., 1999; Albergel et al., 2008). This approach is often applied to depth-extrapolated surface soil moisture time series (e.g., Zhang et al., 2017; Tian et al., 2020). It has also been used to depth-extrapolate surface soil moisture time series derived from CRNS (Peterson et al., 2016) as well as to evaluate the performance of the SMAR model (e.g., Manfreda et al., 2014). This exponential filter has a single calibration factor: the characteristic time length T (days). Although attempts have been made to investigate the controls of T and relating its variability to climatic variables, vegetation characteristics and soil physical properties (e.g., Wang et al., 2017; Bouaziz et al., 2020), the characteristic time length T is commonly treated as bulk calibration parameter which needs to be optimised against reference soil moisture information.

2.3.3 Application of depth-extrapolation approaches

We applied the SMAR model in its original form with aggregated daily soil moisture data by calibrating the V_2 water loss term as a constant value while the remaining soil physical parameters were assigned according to Tab. 1. The modified version of the SMAR model ($SMAR_{modified}$) introduced in this study was applied with the same soil physical parameters but estimating daily V_2 based on eq. 11–14. Consequently, $SMAR_{modified}$ was applied completely without calibration. ~~The calibration and-~~

295 In order to apply and calibrate the exponential filter approach for comparison, the daily surface soil moisture time series was converted to relative saturation by dividing it by the porosity n_1 . The extrapolated second layer time series of relative saturation based on the exponential filter is then converted back to soil moisture by multiplication with the porosity of the second, deeper soil layer n_2 . The same porosity values (Tab. 1) are used as for the application of SMAR and SMAR_{modified}.

The calibration and evaluation was performed against ~~an average reference~~ soil moisture time series in the deeper layer derived from in-situ ~~soil moisture sensors~~. ~~All available in-situ sensor soil moisture time series per depth were averaged to derive average soil moisture time series per sensor depth. Subsequently, we calculated an average soil moisture time series for sensors of the soil moisture sensor network (SMN) covering the entire study period. The reference soil moisture content of the second, deeper soil layer was calculated by weighting the averages per depth individual sensor values according to their representative layer extent (called reference time series in the following).~~ For example, having soil moisture sensors installed in 30, 50 and 70 cm depth, the ~~average~~ soil moisture content per time step ~~of all sensors installed observed~~ in 50 cm is representative for the layer between 40 and 60 cm. The soil physical parameters assigned to the individual layers can be found in Tab. ~~1~~ and were weighted the same way. The calibration is performed by minimising the root-mean square error (RMSE) between the depth-extrapolated soil moisture time series and the entire reference soil moisture time series in of the second soil layer.

310 The original SMAR with calibrated V_2 ~~and~~ the modified SMAR model (SMAR_{modified}) with estimated V_2 ~~are (without calibration) and the exponential filter with calibrated T was~~ applied to estimate a soil moisture time series in a second soil layer with a maximum depth below terrain surface of 70, 130, 200, 300 and 450 cm. ~~In contrast, the modified SMAR model based on eq. 11–14 is applied using the same soil physical parameters but it does not require calibration of the V_2 water loss term.~~

~~In order to test if a better surface soil moisture time series translates to better extrapolated soil moisture values in the second layer, we apply the SMAR model using the CRNS-derived surface soil moisture estimated from the standard transfer function (eq. (1)) as well as using the UTS (eq. (5) – (6)) with the parameter set resulting in the highest goodness-of-fit expressed by the lowest RMSE.~~

~~The vertical extent~~ The depth of the first soil layer ~~is defined according to the representative measurement depth of the CRNS-derived soil moisture time series. In first step, the model is tested using a depth of the first layer of 35 cm as the was~~ set to the median sensitive measurement depth of ~~CRNS is often estimated to range between 30 and 40 cm. However, more accurate approaches exist to determine the sensitive measurement depth. In this study, we also calculate the CRNS method for the study period. We calculated the~~ median CRNS measurement depth of the entire ~~CRNS-soil CRNS-derived soil~~ moisture time series based on Schrön et al. (2017) ~~and use it as the depth of the first soil layer in the SMAR model~~. According to Schrön et al. (2017), the sensitive measurement depth D_{86} is estimated using the calibrated CRNS-derived soil moisture time series for ~~distances from 1 to 300 m around the instrument. Subsequent averaging allows for estimating the average measurement depth in the CRNS footprint for each time step of the time series. The time series median measurement depth D_{86} is then calculated for the soil moisture time series derived with the standard transfer function and the UTS. For both CRNS-derived soil moisture time series, the estimated median sensitive measurement depth is 20 cm and much smaller than the rough initial estimate of 35 cm. As a consequence, we decided to apply the original and modified SMAR model with a first layer depth of both 20 cm~~

330 and 35 cm to investigate the effect on the resulting depth-extrapolated soil moisture time series.

In summary, for each maximum depth of the second soil layer, the SMAR model is applied in its original form based on calibration and in the modified version presented in this study which does not require calibration. This is done using the CRNS surface soil moisture time series based on the standard transfer function as well as on the UTS. Lastly, we test whether the
335 estimation of

The three depth-extrapolation approaches are applied in the representative measurement depth of CRNS and thus, the depth of the first soil layer, has an influence on the resulting modelled soil moisture time series in the second layer. An overview of the different applications of the SMAR model performed in this study is given in Fig. ?? following scenarios:

340 Overview of SMAR models set up in the scope of this study to compare the original SMAR based on the calibration of the water loss V_2 and the modified SMAR which does not require calibration.

Scenario Profile 1 and Scenario Profile 2 Surface soil moisture estimated separately from two individual profiles of in-situ soil moisture sensors (average over the two sensors installed in 10 and 20 cm depth), depth extrapolation calibrated/evaluated against reference second layer soil moisture calculated from the deeper sensors of the each individual sensor profile.

345 To assess the robustness of the modified and uncalibrated SMAR model, we made a simple assessment of parameter uncertainty and its effect on the model results. We set up an ensemble of 50 realizations of the modified SMAR by randomly varying the values for $n_1, n_2, se_1, se_2, sw_2$ and R_1 in a range of \pm

Scenario SMN_{arithmetic} Surface soil moisture estimated with the arithmetic average of all in-situ soil moisture sensors of the SMN (depth-averages of sensors installed in 10 and 20 cm). These sensitivity runs of the modified, uncalibrated SMAR are then assessed using the minimum to maximum range of calculated root mean square error (RMSE) between the simulated soil moisture time series in the second soil layer and the reference from cm depth, 12 and 6 sensors per depth), depth extrapolation calibrated/evaluated against reference second layer soil moisture calculated from the arithmetic depth-averages of all in-situ sensors. In satellite soil moisture estimations, a threshold of $0.06 \text{ cm}^3 \text{ cm}^{-3}$ has been used (Jackson et al., 2010) to evaluate the original SMAR performance for root-zone soil moisture estimates based on satellite-derived surface soil moisture information (Baldwin et al., 2019). We adopt this benchmark for evaluating the performance of the uncalibrated, modified SMAR in this study. of the SMN.

355 Lastly, we performed a full calibration of the original and modified SMAR models in order to estimate the best possible simulation results within a physically acceptable range of the model parameters. This was done by randomly varying the values for $n_1, n_2, se_1, se_2, sw_2$ and R_1 in a range of ± 20

Scenario SMN_{weighted} Weighted average surface soil moisture estimated after Schrön et al. (2017) from all in-situ soil moisture sensors of the SMN in 10, 20 and 30 cm. For the original SMAR model, the water loss term V_2 was calibrated instead of the R_1 with values in the range between 1 and a maximum of 500 mm. The calibration was performed by selecting the parameter combination that resulted in the lowest RMSE among a total of 10,000 random parameter sets. For the full calibration scenarios, we defined the year 2017 as the calibration period, while the entire study period (2016-2022) is used to evaluate the depth-extrapolated cm depth (26 in total), depth-extrapolation calibrated/evaluated against reference second layer soil moisture calculated from the arithmetic depth-averages of all in-situ sensors of the SMN.

365 Scenario CRNS_{Revised standard} Surface soil moisture time series. Except for the fact that several parameters were calibrated, the different scenarios are identical to those where just the V_2 parameter was calibrated (see Fig. ??). In all SMAR applications in this study, the initial soil moisture content of the second layer was set to the first CRNS-derived soil

370 moisture record of the first layer. The SMAR model with physically reasonable environmental value ranges showed generally low performance as described in the results section and led to some additional calibration tests of the model. Experimental calibration runs indicated that calibration parameters in a non-physical value range could produce better model results. Therefore, a second full calibration was performed where the values of the parameters se_1 , se_2 and sw_2 were allowed to range from -1 to their initial, literature-based value while the range for other model parameters remained unchanged from CRNS based on the standard transfer function, depth-extrapolation calibrated/evaluated against reference second layer soil moisture calculated from the arithmetic depth-averages of all in-situ sensors of the SMN.

375 ~~The SMAR model was originally designed to depth-extrapolate surface~~

Scenario CRNS_{UTS} Surface soil moisture time series on a daily resolution, as it assumes that all water above field capacity se_1 infiltrates into the second layer within one day (Manfreda et al., 2014). Consequently, the SMAR model has been applied on a daily resolution in previous studies (e.g., Baldwin et al., 2017, 2019). In CRNS research, an hourly temporal resolution is the community standard and therefore, we test whether the SMAR models in their original and modified forms can also be applied at hourly resolution with a reasonable goodness-of-fit. All analyses described in this chapter are therefore carried out on both a daily and hourly basis. from CRNS based on the UTS, depth-extrapolation calibrated/evaluated against reference second layer soil moisture calculated from the arithmetic depth-averages of all in-situ sensors of the SMN.

380

385 All calculations were performed in R statistical software (R Core Team, 2018, 2023) using the hydroGOF package (Zambrano-Bigiarini, 2017, 2020) for calculating goodness-of-fit measures which evaluate absolute values and time series dynamics, namely the RMSE, the Kling-Gupta-Efficiency (KGE) (Gupta et al., 2009) ~~as well as~~, the Pearson correlation coefficient as well as the Nash-Sutcliffe-Efficiency.

3 Results and discussion

390 3.1 CRNS-derived surface soil moisture time series

The goodness-of-fit of the calibrated CRNS-based soil moisture time series to the time series derived from in-situ point observations is shown for the two transfer functions Tab. 2. When the different transfer functions are calibrated against an arithmetic average soil moisture from soil samples and compared to an arithmetic average of soil moisture time series in 10-30 cm depth, the Pearson correlation coefficient and the KGE are lower than when using a weighted average of soil moisture observations for calibration as proposed by Köhli et al. (2015) and Schrön et al. (2017). However, the RMSE is slightly higher for the calibration against the weighted observations. This might be linked to differences between the laboratory measurements of soil moisture in the soil samples (which were used for calibration) and the continuous soil moisture data obtained from the in-situ sensors. Overall, however, in view of the much better KGE and correlation values, the results underline the importance of the weighting procedures when calibrating the CRNS observations to derive soil moisture estimates or comparing them to observations from in-situ soil moisture sensors.

395

400

Table 2. Goodness-of-fit between the CRNS-derived soil moisture time series and the arithmetic and weighted average soil moisture time series from the local in-situ point-sale soil moisture sensors in 10-30 cm depth. The different neutron to soil moisture transfer functions are independently calibrated against soil moisture from soil samples taken in February 2019. The UTS transfer function can be used with different parameter sets originating from different neutron transport models which are either based on an energy level threshold (thl) or a more realistic detector response functions (drf).

Transfer function	In-situ soil moisture	Calibration parameter [cph]	KGE [-]	RMSE [$\text{cm}^3 \text{cm}^{-3}$]	Pearson correlation [-]
Revised standard		777	0.08	0.030	0.88
UTS URANOS drf		1245	0.14	0.029	0.86
UTS URANOS thl	Arithmetic average	1596	0.59	0.020	0.87
UTS MCNP drf		1294	0.33	0.025	0.87
UTS MCNP thl		1645	0.59	0.021	0.87
Revised standard		809	0.46	0.030	0.91
UTS URANOS drf		1302	0.49	0.029	0.89
UTS URANOS thl	Weighted average	1693	0.81	0.022	0.90
UTS MCNP drf		1357	0.60	0.027	0.90
UTS MCNP thl		1741	0.77	0.023	0.90

The goodness-of-fit of the CRNS-derived soil moisture time series that are based on the revised standard transfer function is always lower than for those that are derived with the UTS all parameters sets, especially when the KGE is considered, showing the improved soil moisture estimation with the UTS. However, the parameters sets of the UTS mimicking the varying sensitivity of a real neutron detector to neutrons of different energies (URANOS drf, MCNP drf) perform worse than those which rely on a simple energy range threshold (URANOS thl, MCNP thl). This counter-intuitive result has been previously described by Köhli et al. (2021) and could be related to the high sensitivity of the CRNS method to the soil moisture dynamics in the first few centimetres of the soil where unfortunately no in-situ sensors are installed (the uppermost sensors are installed in 10 cm depth). Therefore, the better performance of the energy threshold parameters sets of the UTS can be related to insufficient reference soil moisture information from the in-situ sensor network. Generally, the UTS with the parameter sets representing the response of a real neutron detector can be expected to be provide more accurate results. Here, the UTS with parameter set MNCP drf reveals a higher statistical goodness-of-fit compared to the URANOS drf parameter set which is in line with the findings presented in Köhli et al. (2021). The improved performance of the UTS with the parameter set MNCP drf compared to the standard transfer function is shown in Fig. 2, revealing that the latter tends to overestimate soil moisture under the wet winter conditions and underestimate soil moisture under dry summer conditions.

Different from the study of Köhli et al. (2021) which introduced the UTS, we apply UTS to derive soil moisture from neutron observations at a forest site. The UTS calibration parameter N_D represents the average count rate under boundary conditions of the neutron transport simulations conducted to the derive the UTS. Therefore, N_D can be expected to be close to the average

corrected neutron intensity observed at a study site with little or without vegetation or other above-ground hydrogen pools influencing the observed neutron intensity. At our study site, the calibrated N_D is much higher than the observed average
420 corrected neutron intensity N_{pi} (557 cph). This is probably caused by the influence of the forest vegetation on observed neutron intensities and the calibration parameter of the transfer function and has been similarly described for the standard transfer function by Baatz et al. (2015). As hydrogen stored in air humidity influences the functional relationship between neutron intensities and soil moisture, hydrogen stored in vegetation might have a similar effect. Therefore, a correction or inclusion approach for other above-ground hydrogen pools such as vegetation may yield an even better performance of the UTS and may
425 be investigated in future studies.

Our analyses confirm the improved performance of the UTS compared to the standard transfer function. In order to test whether the improved performance in deriving surface soil moisture translates into a better estimation of soil moisture in deeper layers, we apply the SMAR model using the surface soil moisture time series based on both the revised standard transfer function and the UTS with the MCNP drf parameter set (Fig. 2).

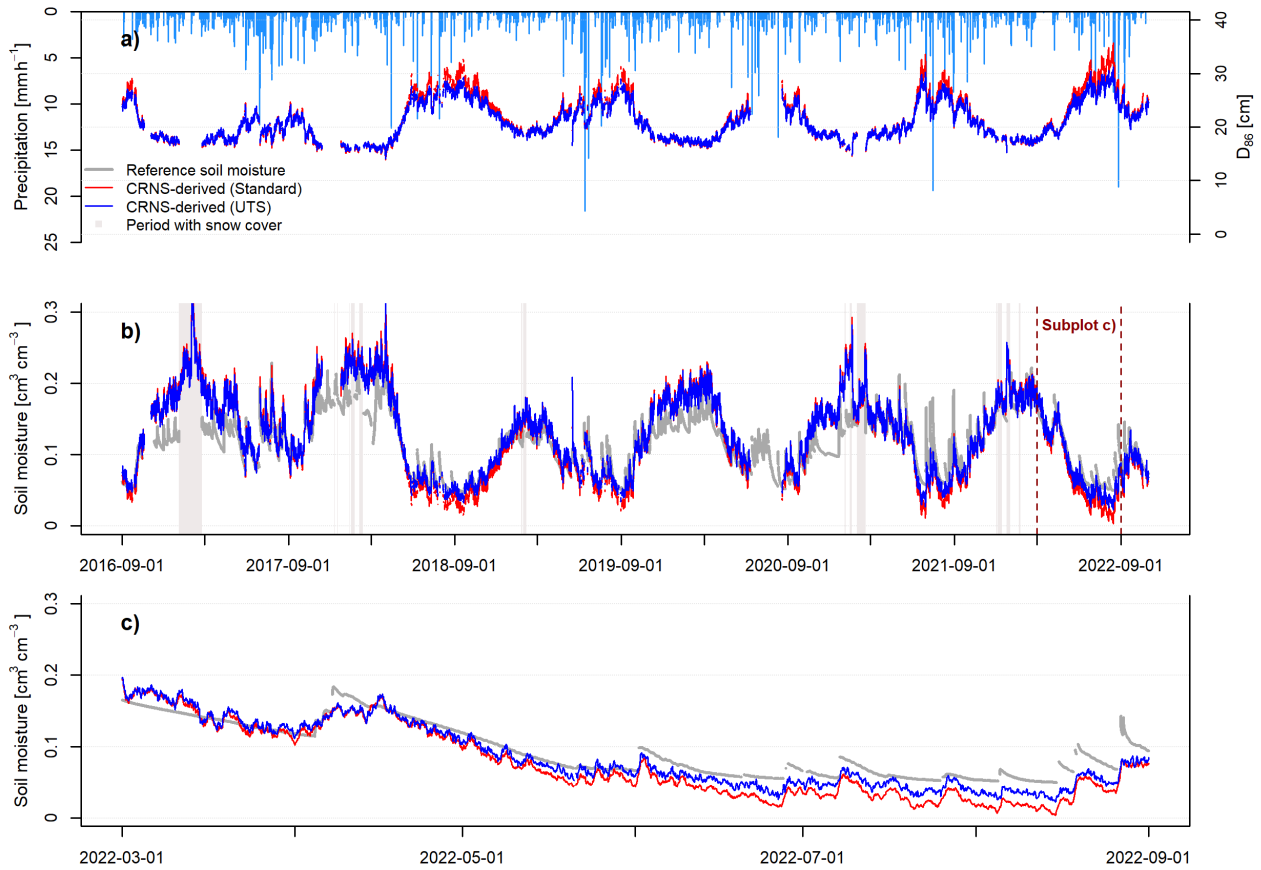


Figure 2. Soil moisture estimates with CRNS. (a) estimated time-variable sensitive measurement depth D_{86} of the CRNS-approach and precipitation time series (light blue bars); (b) soil moisture time series derived with the revised standard transfer function and the UTS with parameter set MCNP drf and (c) a period in 2022 illustrating the differences between the two CRNS-derived soil moisture time series.

3.2.1 Original SMAR with calibrated water loss and uncalibrated, modified SMAR

The performance measures and the corresponding values for the depth-extrapolated soil moisture time series The performance of the different depth-extrapolation approaches, i.e. based on the calibrated original SMAR (calibrated water loss only) and the uncalibrated modified SMAR, the uncalibrated SMAR_{modified} (estimated water loss based on eq. (11-14)) as well as the exponential filter approach (calibrated characteristic time length parameter) for the different scenarios are listed in Tab. ?? as well as Tab. ?? and exemplary time series for a second layer depth of 130 cm are A1- A3 and shown in Fig. 5 and Fig. ?? for a hourly and daily resolution, respectively. The standard transfer function and the UTS produce similar results with RMSE values ranging between 0.055 and 0.015 $\text{cm}^3 \text{cm}^{-3}$ for hourly values and between 0.054 and 0.014 $\text{cm}^3 \text{cm}^{-3}$ for daily values over all simulated scenarios. The SMAR model with daily resolution generally results in a higher goodness-of-fit. The correlation coefficients tend to be lower for the scenarios using the uncalibrated, modified SMAR and higher for the original SMAR with calibrated water loss. For KGE, the results are the opposite.

The better performance at a daily time step (irrespective of the depth-extrapolation method) can be attributed to the fact that it is generally assumed that all water above field capacity infiltrates from the first into the second layer within one time step. While this may be a reasonable assumption on a daily time step for which the SMAR model was designed for (Manfreda et al., 2014), this prerequisite is likely to be violated at the hourly time step. Nevertheless, for our study site, the differences in terms of the RMSE are rather small, indicating that the SMAR model may also be used with an hourly resolution.

Following the RMSE 3. Figure 3 also includes a RMSE threshold of $\leq 0.06 \text{ cm}^3 \text{ cm}^{-3}$ which has been used to evaluate the original SMAR performance (Baldwin et al., 2019; Guo et al., 2023), all simulations with the original and with the modified SMAR and both with an hourly and daily resolution lie in previous studies (Baldwin et al., 2019; Guo et al., 2023). In all scenarios and all depths, with exception of SMAR_{modified} in the Profile 2 scenario, the RMSE of depth-extrapolated time series lies below this threshold. This indicates that all SMAR models, indicating that both SMAR models and the exponential filter approach result in acceptable soil moisture time series for the second soil layer down to 450 cm depth according to RMSE performance. However, taking the dynamic goodness-of-fit parameters KGE and correlation coefficient into account, the performance with regard to indicators more sensitive to temporal dynamics such as the KGE and the NSE show negative values indicating an insufficient simulation of the temporal dynamics is not satisfactory of second layer soil moisture times compared to the reference. This can also be visually identified from seen in Fig. 5 and Fig. ?? for showing the extrapolated soil moisture time series with the different approaches in a second layer with a maximum depth of 130 cm. The original SMAR with calibrated constant water loss reaches the wilting point of the second soil layer over large parts of the study period, indicating that the water loss calibrated by minimizing RMSE, results in a high constant water loss to match the reference average water content of the second layer but thereby causing too strong and rapid decreases of soil moisture in dry summer periods. Here, the uncalibrated, modified SMAR model provides more realistic gradual decreases. For example, comparing the scenarios of Profile 1 and Profile 2, the performance of the individual extrapolation approaches in terms of capturing the temporal soil moisture dynamics can differ strongly. These strong differences and largely unsatisfactory representation of soil moisture ;

465 leading to a better performance when visually assessing the time series. This is also true for the maximum second-layer depth of 450 cm investigated dynamics indicates that the RMSE threshold used in previous studies to evaluate the performance of depth-extrapolation approaches should be treated with caution. Regarding the exponential filter method, it should be noted that the maximum T value of 300 days defined in this study (was reached during calibration in some scenarios as displayed in Fig. ?? and 4.

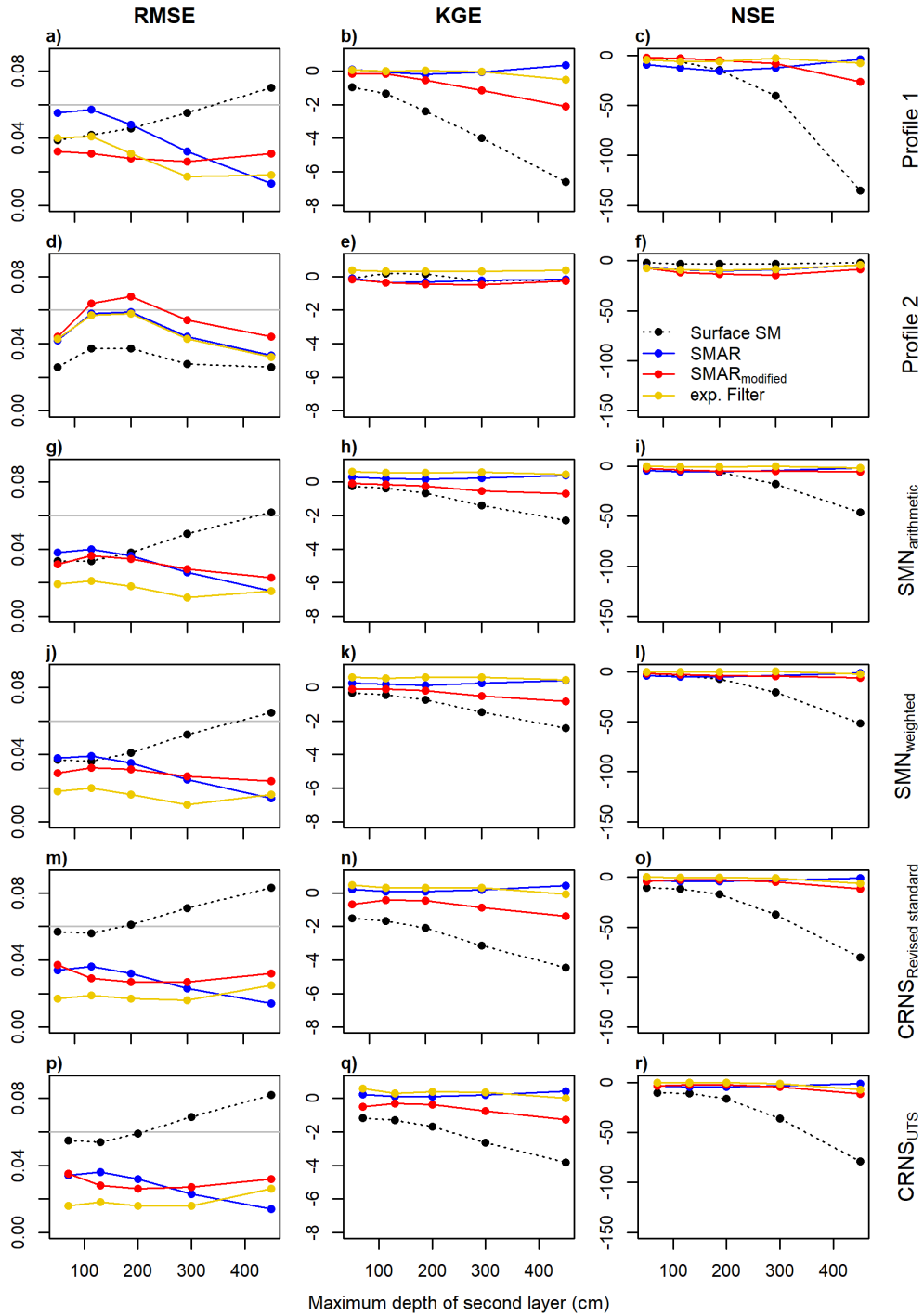


Figure 3. Goodness-of-fit parameters derived for the depth-extrapolation approaches in the individual scenarios depending on maximum second layer depths. In addition to the three depth-extrapolation methods applied in this study, also the comparison with the surface soil moisture time series is shown. For the RMSE, a threshold value $0.06 \text{ cm}^3 \text{ cm}^{-3}$ is indicated as grey horizontal line.

Fig. ??) and illustrates that care should be taken when relying on statistical 3 also shows the goodness-of-fit measures and
470 that a visual assessment and interpretation of the simulation results should be undertaken. Nevertheless, it should be noted that
the simulated parameters between surface soil moisture time series both for the original and for the modified SMAR do not
represent intermediate pulses of increased soil moisture seen in the reference data even during the drier summer period.

For large maximum depths of the second layer such as 450 cm, the original SMAR with calibrated water loss better simulates
the amplitudes of of the respective scenario and the reference soil moisture time series in the second soil layer in order to test
475 if any of the depth-extrapolations perform better than simply assuming that the soil moisture in the second layer for a temporal
resolution of both hours and days. This indicates that the water loss estimated with the modified SMAR is too low for large
depths. The condition of eq. (13), imposing that no evapotranspiration losses occur when water percolates from the first to
the second layer, could be one reason. Another reason could be uncertainties of the relative root fraction that is required to
scale the water losses from the the first to the second layer. The use of an exponential model to describe the cumulative root
480 distribution, as done in this study, is highly simplistic and such models generally remain under debate (e.g. Pierret et al., 2016)
. Furthermore, too much water percolating from the first into the second soil layer may be compensated through the calibration
of the water loss parameter in the original SMAR model, but this cannot be done when the uncalibrated, modified SMAR is
applied.

Another major reason for the generally poor performance of both the original and the modified SMAR can be the literature-based
485 soil physical parameters used here in order to apply the SMAR model without calibration against in-situ reference measurements.
In ensemble simulations with the modified SMAR, the soil physical parameters were varied in a range of $\pm 10\%$. The minimum
and maximum RMSE values derived from the 50 hourly and daily ensemble runs are shown in Tab. ???. It can be seen that
smaller RMSE values can be achieved with parameter values that are different from the initial ones (Tab. ??). The maximum
RMSE for all depths except for 70 cm still meet the RMSE benchmark criterion, indicating a certain robustness of the is similar
490 to the surface soil moisture time series. However, all depth-extrapolation approaches, including the uncalibrated, modified
SMAR model presented in this study if the soil physical parameters can be reasonable well estimated.

We also tested the impact of the input SMAR_{modified}, show a better performance in most scenarios and especially in larger
depths. This indicates that if no reference soil moisture time series for calibration in the depth of interest is available, the
uncalibrated SMAR_{modified} provides better results than simply using the available surface soil moisture time series to both
495 the original SMAR with calibrated water loss and the uncalibrated, modified SMAR. Using either the CRNS-derived as a first
estimate for the soil moisture time series based on the UTS equation or the revised standard equation for the first layer results
in visually similar results with similar RMSE values, slightly higher correlation coefficients for the second case, and slightly
better KGE values for the first case (Tab. ??, Tab. ??). Overall, in this study, a better estimated in a second, deeper layer of
interest. An exception to this finding is scenario Profile 2, where the NSE and RMSE of all depth-extrapolation approaches
500 perform worse compared to using the surface soil moisture time series from CRNS does not necessarily translate into a
distinct improvement of the depth-extrapolated time series. This may be explained by the considerable overall deficiencies of
the SMAR models to represent the soil moisture dynamics at our study site which are larger than the differences between as the

predicted time series in the second soil layer. Comparing the scenarios Profile 1 and Profile 2 in Fig. 5 shows large differences in the surface soil moisture time series derived with the different neutron-to-soil moisture transfer functions.

505 ~~In contrast, improvements of the depth-extrapolated soil moisture times between the two scenarios but a rather similar reference soil moisture time series in the second layer can be seen when the depth of the top soil layer in the SMAR model is taken to be the median calculated sensitive measurement depth (D_{86} , Schrön et al. (2017)) of the CRNS technique. Here, the statistical goodness-of-fit is generally higher compared to using an assumed sensitive depth of 35 cm for the top soil layer. This is the case for both the standard and the modified SMAR model and independent of the transfer function used for the CRNS soil~~

510 ~~moisture in the top layer (standard or UTS) with hourly and daily resolution. The better matching time series compared to the reference time series is also visible in Fig. 5 and Fig. ?? and is expressed through the RMSE values in Tab. ?? and Tab. ?. The nature of the SMAR model as a water balance approach implies that the correct estimation of the volume of the upper soil layer and its storage is directly related to the accuracy of the depth-extrapolated time series of the second soil layer. Consequently, an accurate assessment of the sensitive measurement depth of CRNS is also highly important when using CRNS-derived~~

515 ~~soil moisture time series in soil layer. This indicates small scale heterogeneity of surface soil moisture within the SMN caused by e.g. heterogeneous infiltration, root-water uptake and preferential flow processes. Preferential flow in macropores including bypass flow along roots (e.g., Nimmo, 2021) can result in highly conductive forest soils with infiltrating water being quickly transported from the surface to deeper layers and bypassing e.g. individual point-scale sensors. Heterogeneous evapotranspiration, interception, (e.g., Schume et al., 2003) and root distribution patterns (e.g., Jost et al., 2012) add to the surface~~

520 ~~soil moisture heterogeneity in forests which may explain the differing performance of all depth extrapolation approaches at different individual profiles of in-situ soil moisture sensors. In larger depths with e.g. (soil-)hydrological model applications, lower root-densities, more similar soil moisture dynamics can be expected, explaining the more similar soil moisture dynamics between the two individual sensor profiles. When assessing the results obtained from using the in-situ sensor, it should also be noted that the use of the manufacturer's calibration function adds additional uncertainty to the results.~~

525 ~~Statistical goodness-of-fit between the depth-extrapolated hourly soil moisture time series from CRNS surface observations and the average soil moisture time series in the second layer calculated from the available in-situ point-scale soil moisture sensors. The water loss parameter is either a calibrated static value (original SMAR model) or estimated based on the procedure described for the modified SMAR model, see chapter 2.~~

Hourly depth-extrapolated soil moisture time series for a depth of 130 cm using the calibrated standard SMAR model (calibrated water loss V_2) with a top layer depth of 35 cm (a), and 20 cm (b) as well as the depth-extrapolated soil moisture time series based on the uncalibrated modified SMAR (estimated water loss) model presented in this study (top layer depth of 35 cm (c) and 20 cm (d)) based on the CRNS-derived surface soil moisture time series from the standard transfer function and the UTS:

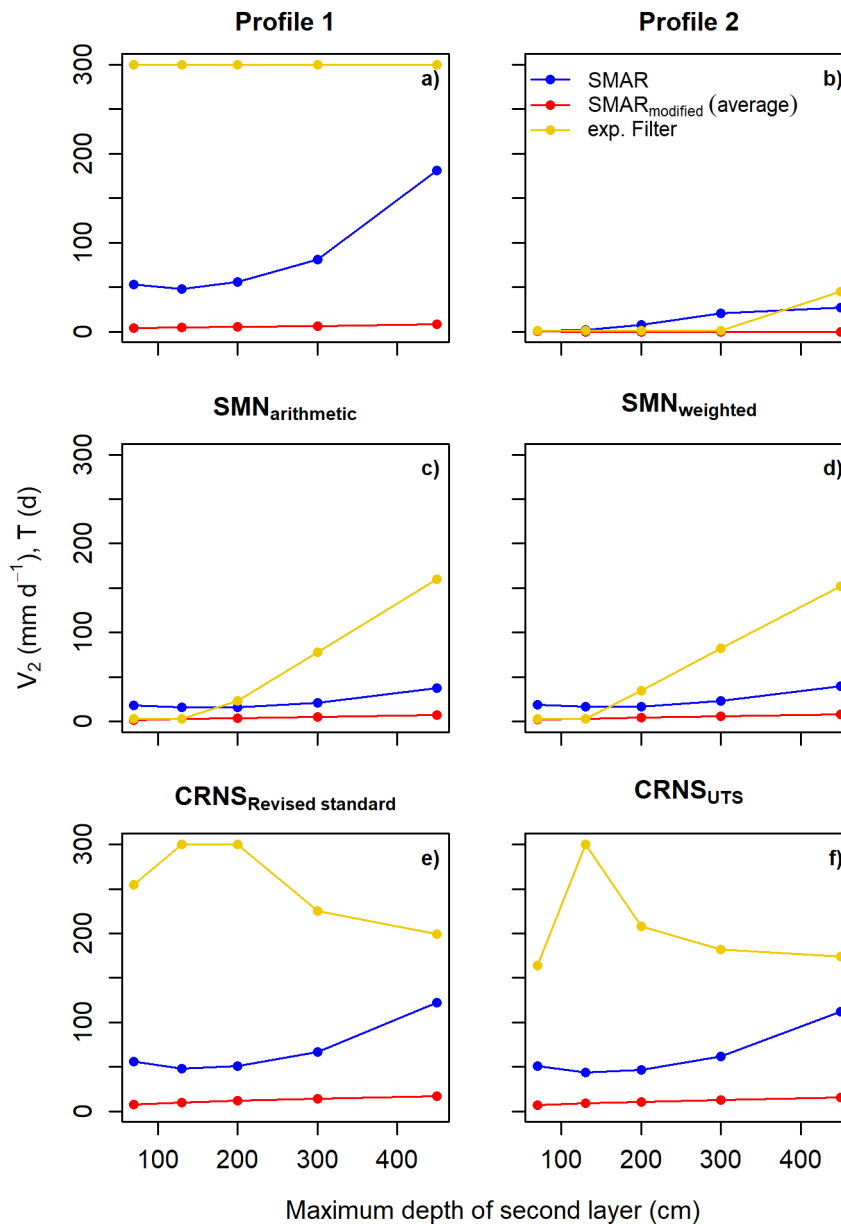


Figure 4. Optimum calibration parameters (minimum RMSE) derived for the different extrapolation approaches and depths in the individual scenarios. For SMAR_{modified} the time series average of V_2 is shown.

530 *Daily* depth-extrapolated soil moisture time series for a depth of 130 cm using the calibrated standard SMAR model (calibrated water loss V_2) with a top layer depth of 35 cm (a), and 20 cm (b) as well as the depth-extrapolated soil moisture time series based on the uncalibrated modified SMAR (estimated water loss) model presented in this study (top layer depth of 35 cm (c) and 20 cm (d)) based on the CRNS-derived surface soil moisture time series from the standard transfer function and the UTS.

535 Statistical goodness-of-fit between the depth-extrapolated *daily* surface soil moisture time from CRNS and the average soil moisture time series in the second layer calculated from the available in-situ point-scale soil moisture sensors. The water loss parameter is either as a calibrated static value (original SMAR model) or estimated based on the procedure described in the methods section (modified SMAR model, see chapter 2).

3.2.1 Full calibration of the original and modified SMAR

540 To further assess the performance of the original and modified SMAR at the study site, we performed a full (all parameter) calibration of the two SMAR models with 10,000 random combinations of the soil physical parameters. The initially assigned soil physical parameters were altered in the range of $\pm 20\%$ to assign values in a physically acceptable range for the sandy soils at the study site. Additionally to the soil physical parameters, the bulk water loss V_2 in the original SMAR was calibrated with random values in the range from 1 to 500 mm. For the modified SMAR model, the relative root fraction in the first layer R_f was varied in the range of $\pm 20\%$ instead.

545 The results of the full calibration can be found in Tab. ?? and Tab. ?? and exemplary time series for a second layer depth of 130 cm are [Using averages of in-situ soil moisture sensor networks therefore improve the performance of all depth-extrapolation approaches](#) as shown in Fig. ?? and Fig. ?? for a hourly and daily resolution, respectively. The results for the maximum depth of 450 cm can be found in the appendix. As expected, minimizing the RMSE in the calibration period 2017 leads to a decrease of the RMSE for the entire study period compared to the uncalibrated modified SMAR or when calibrating the water loss term in the original SMAR only. This is the case for both the hourly and daily time step, with generally better performance for the latter in terms of RMSE and KGE. Using a first layer depth of 20 cm instead of 35 cm leads to better soil moisture dynamics in the deeper layers. This is in line with results presented in the previous chapters when comparing the uncalibrated, modified SMAR and the original SMAR with calibrated water loss.

555 Following the statistical goodness-of-fit parameters in Tab. ?? and Tab. ??, [6. Scenarios \$SMN_{arithmetic}\$ and \$SMN_{weighted}\$](#) as well as both CRNS scenarios generally show a higher goodness-of-fit for most depth-scaling approaches. This highlights [the need for a representative estimation of surface soil moisture at complex study sites with strong small-scale heterogeneities in soil moisture and soil hydrological processes when depth-extrapolating surface soil moisture time series and underlining the potential of CRNS.](#) The differences between $SMN_{arithmetic}$ and $SMN_{weighted}$ are rather small, indicating only a minor impact of using a weighted surface soil moisture time series and comparing it to a reference second layer soil moisture time series calculated from arithmetic averages. Similarly, [the modified SMAR performs worse than the calibrated original SMAR in different depths after all parameters have been calibrated](#) [difference between \$CRNS_{Revised\ standard}\$ and \$CRNS_{UTS}\$ is relatively small with a slightly higher goodness-of-fit in the scenario \$CRNS_{UTS}\$.](#) However, as the differences are small, a clear conclusion [that a better CRNS-derived surface soil moisture time series translates into a better depth-extrapolated time series cannot be](#)

drawn from the results of this study. This may be attributed to using a single-objective optimization for minimizing the RMSE, only. Furthermore, in the original SMAR, the bulk water loss from the second layer was optimized while for the modified SMAR, only the cumulative root fraction in the first layer was adjusted. This leads to more restricted conditions for the modified SMAR model. For example, calibrating the estimated complete water loss in the latter eq. 11 based on a calibration factor could lead to improved the results of the fully calibrated, modified SMAR and more close to those derived for the fully calibrated original SMAR. Nevertheless, the generally higher process restrictions due to the defined estimation of ET_2 and P_2 in eq. 13–14 of also be linked to the modified SMAR remain. differences in the CRNS-derived surface soil moisture time series being smaller than the uncertainties introduced by the different depth-extrapolation approaches.

In summary, the full calibration of the original and modified SMAR model with soil model parameters in physically reasonable value range show similar characteristics to those scenarios described in the previous chapter where literature-based values were assigned for soil physical parameters and only the bulk water loss V_2 was calibrated. Although the overall visual performance improved and a higher statistical

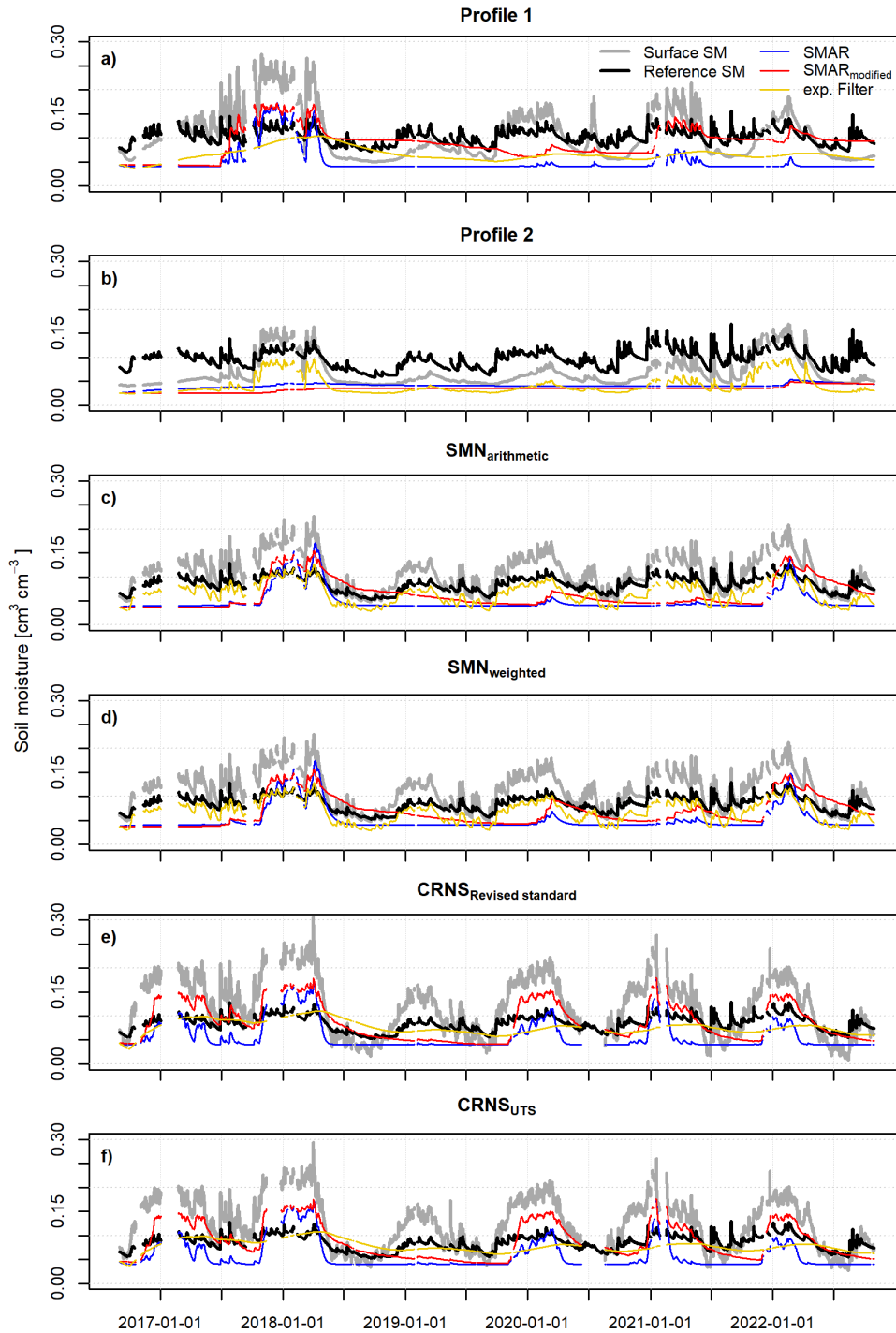


Figure 5. Daily depth-extrapolated soil moisture time series of the different scenarios and depth-extrapolation approaches for a depth of 130 cm. The respective surface soil moisture time series for the first soil layer (0-20 cm) and the reference soil moisture time series for the deeper, second soil layer (20-130 cm) are also shown.

575 In contrast, larger differences can be found between the SMN-scenarios ($SMN_{arithmetic}$ and $SMN_{weighted}$) and the CRNS-scenarios
($CRNS_{Revised\ standard}$ and $CRNS_{UTS}$) where the latter two often show lower goodness-of-fit ~~can be achieved when all~~
~~environmental model parameters are calibrated,~~ parameters for the different extrapolation approaches as expressed by e.g.
a lower KGE. This can be related to general differences between the surface soil moisture derived from the SMN and CRNS
and could be related to the sensor locations of the SMN not being representative for the sensitive measurement footprint of
580 CRNS. Also, the changing sensitive measurement depth of CRNS with soil moisture content may cause uncertainties when
using a constant (median) sensitive measurement depth of 20 cm for the extent of the first soil layer in the ~~original and modified~~
~~SMAR model tested in this study do not show satisfying results with respect to the temporal dynamics of the soil moisture time~~
~~series of the second layer. Many intermediate rainfall events are not captured and thus, the reference soil moisture time series~~
~~show a more dynamic behavior than those simulated by the original and modified SMAR.~~ ~~depth-extrapolation approaches.~~
585 Although this effect may be small, particularly on the daily time step, smoothing hourly CRNS data prior estimating surface
soil moisture and aggregating daily soil moisture estimates could contribute to the poorer performance of depth-extrapolated
time series in the CRNS scenarios compared to the SMN scenarios.

Calibration experiments revealed that assigning values in a non-physical parameter range, e.g., negative values, for soil
physical model parameters could lead to an improved performance of SMAR. When allowing a non-physical value range for
590 the model parameters sc_1 , sc_2 and sw_2 , the visual and statistical performance of both, the original and modified SMAR improve
dramatically with the exception of the depth of 70 cm. Again exemplary shown for a maximum depth of 130 ~~Averaged over all~~
~~tested scenarios, all three depth-extrapolation approaches do not properly represent the time series dynamics the our study site~~
~~as indicated by negative mean NSE values and 450cm depth and both temporal resolutions, KGE values below 0.5 (Fig. ??—~~
~~?? as well as Tab. ?? — ?? illustrate the improved performance of both SMAR models. The poor and even worse performance~~
595 in the depth of 70 cm compared to the full calibration with physically reasonable values could be related to a non-sufficient
value range for the calibrated parameters when values in a non-physically based value range are assigned. Even better results
may also be derived for other depths with a different value range or by also calibrating the remaining parameters n_1 , n_2 , V_2 and
 R_1 in a non-physically reasonable value range. These results show that satisfactory results with the original and the modified
SMAR can be obtained at our study site at the expense of physical realism of the model, and only if in-situ soil moisture
600 measurements in the depth of interest are available for calibration⁷). The highest average goodness of fit is obtained when
applying the exponential filter approach calibrated against reference soil moisture measurements in the second soil layer of
interest. The uncalibrated $SMAR_{modified}$ shows average RMSE and NSE values lying largely between the exponential filter
approach and the calibrated SMAR in its original form, indicating that the introduced $SMAR_{modified}$ can compete with the
(calibrated) original SMAR and can be applied without calibration to derive first estimates of soil moisture in a second, deeper
605 layer.

3.2.1 General discussion

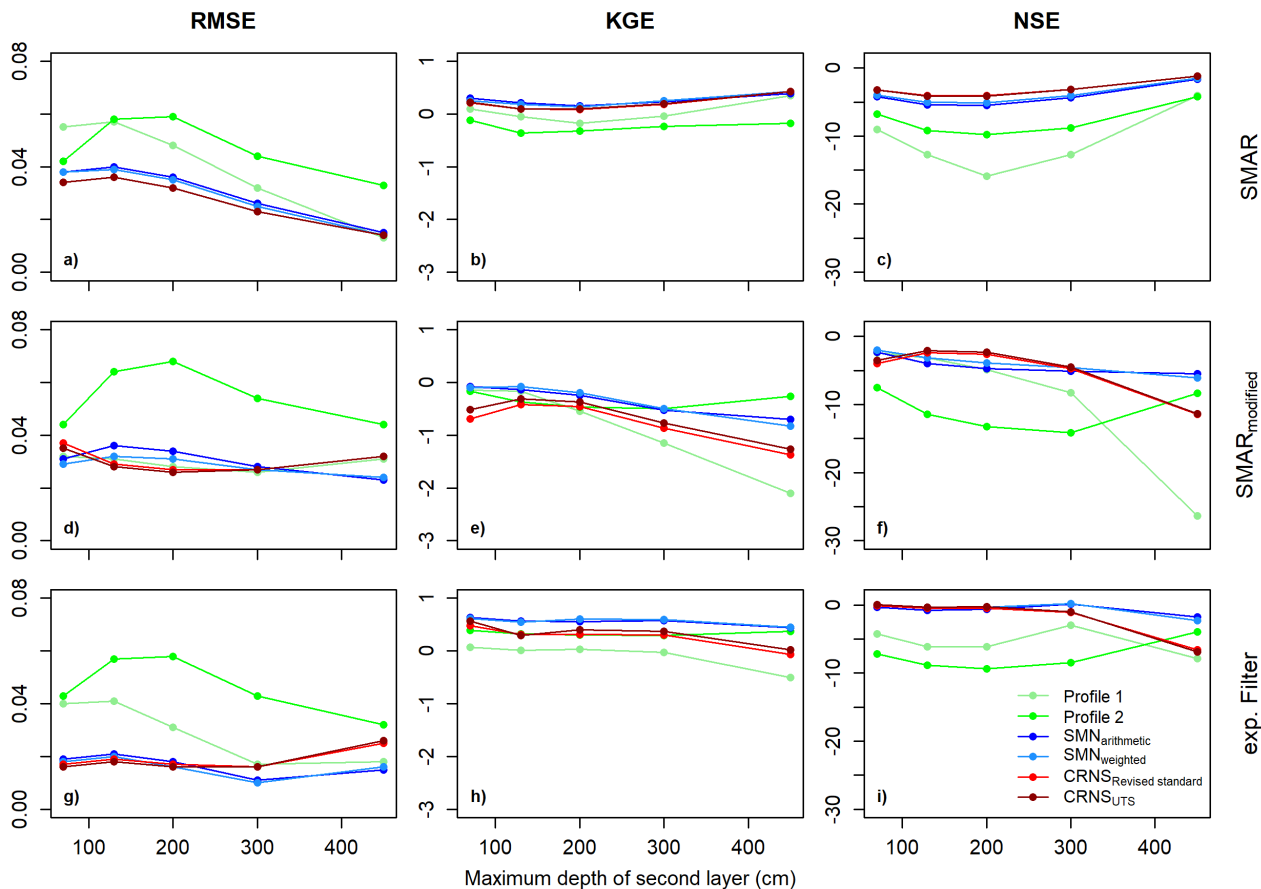


Figure 6. Goodness-of-fit parameters per depth-extrapolation approach and maximum second layer depth for the individual scenarios.

The evaluation of the original SMAR model against in-situ observations in previous studies showed a range of RMSE values and correlation coefficients (e.g., Manfreda et al., 2014; Faridani et al., 2017), indicating that the performance of the SMAR model varies between study sites.

610 Nevertheless, all three approaches do not produce satisfactory results in terms of soil moisture dynamics which may be explained with the particular water flow dynamics at our study site located in a mixed forest with sandy soils ~~may explain the overall unsatisfactory representation of soil moisture dynamics of the SMAR model when model parameters are assigned in a physically reasonable range. Preferential flow in macropores including bypass flow along roots (e.g., Nimmo, 2021) can result in highly conductive forest soils with infiltrating water being quickly transported from the surface to deeper layers. For example, Chandler et al. (2018) and Alaoui et al. (2011) found that forest soils can have higher saturated hydraulic conductivity compared to other land cover types and combined with differing preferential flow processes this may lead to increased infiltration and percolation into lower layers of forest soils (e.g., Alaoui et al., 2011).~~ Complex preferential flow and infiltration processes are unlikely to be properly captured by ~~the SMAR as it allows~~ any of the three depth-extrapolation approaches. This is especially

615

true for SMAR and SMAR_{modified} as they allow water movement only for soil moisture conditions above field capacity. A
620 ~~more complex root distribution than the exponential one assumed in this study and related temporally varying transpiration~~
~~water losses from different depths adds for complexity that is not captured by the SMAR model. Maysonave et al. (2022)~~
~~, for instance, found that root water uptake in forests can vary with time and depth depending on the water availability in~~
~~different layers. These features can neither be reproduced by the original nor modified SMAR and makes forest sites generally~~
625 ~~challenging, in particular for simplified models. However, this may be partly compensated for when model-specific effective~~
~~parameters are used. In this case, calibration against in-situ reference soil moisture information is required and the parameters~~
~~lose their physical meaning and interpretability but may account for the particular soil hydraulic processes of the study site.~~

~~In addition to the simplicity of the model, the field-scale approach of this study adds further difficulties when evaluating~~
~~the simulated soil moisture time series against point-scale soil moisture observations. The reason is their high spatio-temporal~~
~~variability, especially in forests caused by~~ In contrast, the exponential filter includes a constant dependence between the surface
630 soil moisture dynamics of the first and of the deeper, second layer, which could be an explanation for its higher average
performance at our study site with expected highly conductive soils due to e.g. heterogeneous evapotranspiration, interception,
(e.g., Schume et al., 2003) and root distribution patterns (e.g., Jost et al., 2012). Even more preferential flow processes. In addition,
~~the decreasing number of reference in-situ soil moisture sensors with increasing soil depth may lead to a lower representative-~~
~~ness of the reference soil moisture time series at larger depths, lowering comparability to the model results. Nevertheless~~ However,
635 with point sensors installed down to 450 cm, this study allows for exploring the potential of SMAR for larger depths than usually
feasible. Even when depths down to 450 cm are considered, the original and modified SMAR meet the benchmark RMSE of
 $\leq 0.06 \text{ cm}^3 \text{ cm}^{-3}$ in scenarios with literature-based and with calibrated model parameters. This underlines the usefulness of
SMAR to derive a first estimate of soil moisture in a second, deeper soil layer. simple depth-extrapolation approaches for larger
soil depths than commonly applied.

640 ~~The largest~~ An important limitation of the present study for evaluating the standard and the introduced modified SMAR
models is its application to a single observation site. ~~A comparison with other simple depth-extrapolation approaches including~~
~~the soil water index (e.g., Wagner et al., 1999; Albergel et al., 2008); Furthermore, other~~ empirical approaches such as regres-
sion models (e.g., Zhang et al., 2017) and cumulative distribution function matching (e.g., Gao et al., 2018) as well as other
versions of the SMAR model (e.g., Faridani et al., 2017) would allow for an improved evaluation of the presented modification
645 of the SMAR model and should be assessed in future studies at sites with a broader range of climatic conditions, vegetation
covers and soils.

~~Statistical goodness-of-fit between the depth-extrapolated hourly surface soil moisture time series from CRNS and the~~
~~average soil moisture time series in the second layer calculated from the available in-situ point-scale soil moisture sensors with~~
~~the fully calibrated SMAR in a physically acceptable parameter range. The calibrated model parameters and goodness-of-fit~~
650 ~~indicators for the original and modified SMAR model are shown.~~

~~Daily depth-extrapolated soil moisture time series for a depth of 130 cm using the standard SMAR model with a top layer~~
~~depth of 35 cm (a), and 20 cm (b) as well as the depth-extrapolated soil moisture time series based on the modified SMAR~~
~~model presented in this study (top layer depth of 35 cm (c) and 20 cm (d)) based on the CRNS-derived surface soil moisture~~

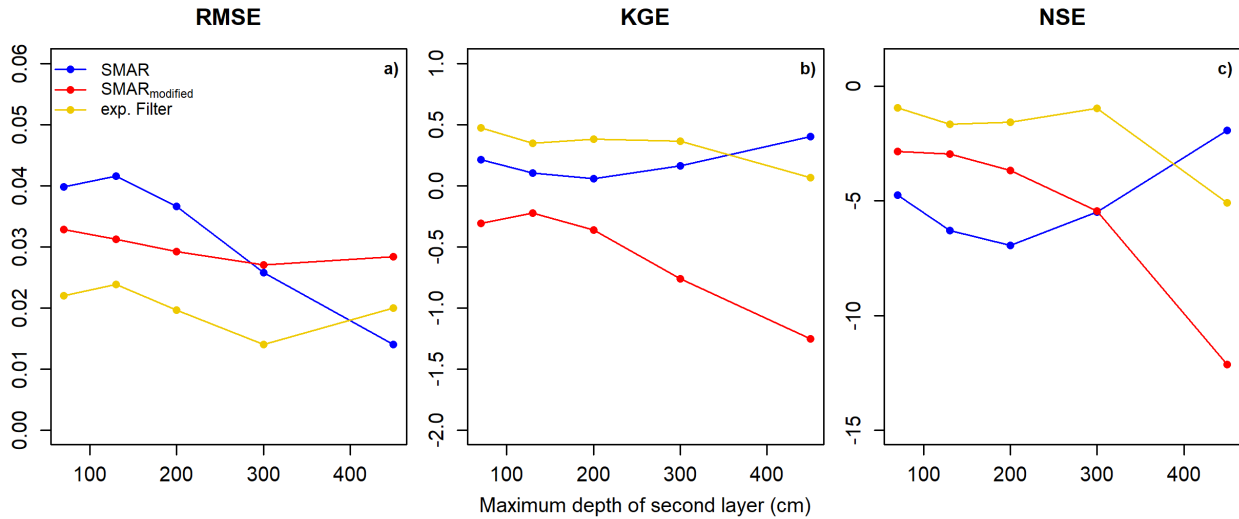


Figure 7. Hourly depth-extrapolated soil moisture time series for a depth Goodness-of-fit parameters of 130 cm using the standard SMAR model with a top layer depth of 35 cm (a), and 20 cm (b) as well as the depth-extrapolated soil moisture time series based on the modified SMAR model presented in this study (top layer depth of 35 cm (c) and 20 cm (d)) based on the CRNS-derived surface soil moisture time series from the standard transfer function and the UTS three depth-extrapolation approaches averaged over all scenarios. The soil physical parameters n_1 , n_2 , sc_1 , sc_2 , sw_2 and R_f were optimized by reducing the RMSE against reference soil moisture values in the year 2017. For the original SMAR model, the water loss term V_2 was calibrated instead of R_f .

time series from the standard transfer function and the UTS. The soil physical parameters n_1 , n_2 , sc_1 , sc_2 , sw_2 and R_f were
 655 optimized by reducing the RMSE against reference soil moisture values in the year 2017. For the original SMAR model, the
 water loss term V_2 was calibrated instead of R_f .

Statistical goodness-of-fit between the depth-extrapolated *daily* surface soil moisture time from CRNS and the average soil
 moisture time series in the second layer calculated from the available in-situ point-scale soil moisture sensors with the fully
 calibrated SMAR in a physically acceptable parameter range. The calibrated model parameters and goodness-of-fit indicators
 660 for the original and modified SMAR model are shown.

4 Conclusions

In the present study we investigated the feasibility of depth-extrapolating surface soil moisture time series derived from CRNS
 to deeper soil layers without additional in-situ soil moisture information for calibration. We furthermore evaluated the Universal
 Transport Solution (UTS) for the estimation of field scale soil moisture from CRNS neutron counts.

665 Being among the first who evaluate the UTS as a new transfer function to estimate field-scale surface soil moisture infor-
 mation from CRNS, we confirm its improved performance compared to the standard approach. The UTS accounts for the
 interdependence of soil moisture and air humidity on the observed neutron intensity, being most important for dry soil condi-

tions. Although applied at a forested site with rather dry soils but with large amounts of above-ground hydrogen stored in the local biomass and influencing the neutron signal, CRNS-derived soil moisture estimates can be improved compared to using established transfer functions. Thus, our results suggest that the UTS should be used for an improved estimation of surface soil moisture in future CRNS research and applications.

We modified SMAR for estimating soil moisture time series in a second, deeper layer in a way that it can be applied without calibration against in-situ sensors and with soil physical properties and the cumulative root fraction as a vegetation parameter only. Our analyses show that ~~for a benchmark RMSE of $\leq 0.06 \text{ cm}^3 \text{ cm}^{-3}$ on average,~~ the uncalibrated ~~modified SMAR~~ SMAR_{modified} can compete with the original SMAR model down to a maximum depth of the second soil layer of 450 cm when the same soil physical properties are assigned and only the water loss term is calibrated. ~~A certain robustness of the uncalibrated, modified SMAR in terms of the RMSE was shown by sensitivity runs of the model. However~~ However, depending on the tested scenario, major temporal dynamics of the reference in-situ soil moisture in the second soil layer are neither captured by the original nor by the modified SMAR nor by the exponential filter approach. This is likely linked to the location of the study site ~~in a mixed forest site; a forest~~ in a mixed forest site: a forest with sandy soils, ~~accompanied with which results in soil moisture being influenced by processes such as~~ preferential flow and root water uptake ~~processes that.~~ These processes are difficult to simulate, especially with rather simple modeling approaches. ~~Only the use of SMAR with calibrated effective albeit non-physical parameters partly accommodates to the specific soil hydraulic processes at the study site, showing an improved simulation of soil moisture dynamics in a~~ On average, the calibrated exponential filter method performed best in predicting soil moisture in a deeper, second soil layer. ~~Under these circumstances, deeper soil moisture time series may be more satisfactorily simulated even with simple modeling approaches such as SMAR.~~

Although our study suggests that improved surface soil moisture estimates from CRNS do not translate to distinctly improved soil moisture estimates in greater depths, a more accurate estimation of the representative measurement depth of CRNS leads to better results of ~~the SMAR model~~ either depth-extrapolation approach. This indicates that an accurate estimation of the representative measurement depth of CRNS is especially important when using CRNS data as input for hydrological models.

Given the overall performance of the SMAR model at our single study site, further research and testing of the presented modified version of the SMAR model with and without calibration at sites with varying climatic conditions, vegetation cover and soil properties is necessary and encouraged for future studies. Despite the overall unsatisfactory performance of the SMAR model with respect to accurately capturing soil moisture dynamics at our study site, ~~meeting it meets~~ the defined RMSE benchmark ~~, of $\leq 0.06 \text{ cm}^3 \text{ cm}^{-3}$ and~~ the simple modification of the SMAR algorithm may serve as a valuable first estimate of soil moisture from a second, deeper soil layer, when in-situ reference soil moisture information for calibration are not available and the soil physical parameters can be reasonably well estimated.

In CRNS research, this modified SMAR approach opens up potential for roving CRNS, i.e., by mounting CRNS instruments on cars (e.g., Schrön et al., 2018a) or trains (e.g., Schrön et al., 2021; Altdorff et al., 2023) moving beyond the field-scale of stationary CRNS applications, thereby providing valuable information for landscape water balancing or hydrological catchment models on larger scales. Moreover, the modified SMAR approach introduced in this study is not limited to CRNS applications.

It may also be used in estimating root-zone soil moisture in greater depths from satellite derived surface soil moisture ~~in which~~ where the original SMAR already proved useful (e.g., Baldwin et al., 2017, 2019; Gheybi et al., 2019).

Data availability. All data sets are available from the authors upon request.

705 **Appendix A**

Table A1. Minimum and maximum RMSE values Statistical goodness-of-fit between the depth-extrapolated daily surface soil moisture time from CRNS using the modified SMAR model of the 50 ensemble runs series and the reference soil moisture time series in the second layer calculated extending from the available in-situ point-scale soil moisture sensors 20 to 70 cm and 130 cm for the simulations with hourly and daily-resolution different scenarios. Asterisk indicates reaching the maximum allowed characteristic time length T value during calibration of the exponential filter method.

Layer 2 extent [cm]	Scenario	Extrapolation approach	Calibration	V_2 [mm d ⁻¹]	T [d]	RMSE [cm ³ cm ⁻³]	KGE [-]	NSE [-]
20-70	Profile 1	SMAR	Yes	1	-	0.055	0.091	-9.066
		SMAR _{modified}	No	-	-	0.032	-0.142	-2.363
		exp. Filter	Yes	-	1	0.040	0.068	-4.240
	Profile 2	SMAR	Yes	53	-	0.042	-0.115	-6.785
		SMAR _{modified}	No	-	-	0.044	-0.161	-7.489
		exp. Filter	Yes	-	300*	0.043	0.338	-7.208
	SMN _{arithmetic}	SMAR	Yes	18	-	0.038	0.297	-4.221
		SMAR _{modified}	No	-	-	0.031	-0.079	-2.309
		exp. Filter	Yes	-	3	0.019	0.634	-0.305
	SMN _{weighted}	SMAR	Yes	19	-	0.038	0.252	-3.958
		SMAR _{modified}	No	-	-	0.029	-0.102	-2.022
		exp. Filter	Yes	-	3	0.018	0.619	-0.097
	CRNS _{Revised standard}	SMAR	Yes	56	-	0.034	0.210	-3.202
		SMAR _{modified}	No	-	-	0.037	-0.063	-3.997
		exp. Filter	Yes	-	255	0.017	0.480	-0.090
	CRNS _{UTS}	SMAR	Yes	51	-	0.034	0.217	-3.252
		SMAR _{modified}	No	-	-	0.035	-0.517	-3.479
		exp. Filter	Yes	-	164	0.016	0.570	0.062
20-130	Profile 1	SMAR	Yes	48	-	0.057	-0.055	-12.754
		SMAR _{modified}	No	-	-	0.031	-0.163	-3.130
		exp. Filter	Yes	-	300*	0.041	0.017	-6.113
	Profile 2	SMAR	Yes	2	-	0.058	-0.363	-9.163
		SMAR _{modified}	No	-	-	0.064	-0.370	-11.418
		exp. Filter	Yes	-	1	0.057	0.324	-8.846
	SMN _{arithmetic}	SMAR	Yes	16	-	0.040	0.021	-5.396
		SMAR _{modified}	No	-	-	0.036	0.093	-3.991
		exp. Filter	Yes	-	3	0.021	0.563	-0.79
	SMN _{weighted}	SMAR	Yes	17	-	0.039	0.181	-5.069
		SMAR _{modified}	No	-	-	0.032	-0.081	-3.116
		exp. Filter	Yes	-	3	0.02	0.546	-0.508
	CRNS _{Revised standard}	SMAR	Yes	48	-	0.036	0.093	-4.086
		SMAR _{modified}	No	-	-	0.029	-0.422	-2.387
		exp. Filter	Yes	-	300*	0.019	0.318	-0.496
	CRNS _{UTS}	SMAR	Yes	44	-	0.036	0.093	-4.140
		SMAR _{modified}	No	-	-	0.028	-0.310	-2.083
		exp. Filter	Yes	-	300*	0.018	0.295	-0.302

Hourly depth-extrapolated soil moisture time series for a depth of 450 cm using the calibrated standard SMAR model (calibrated water loss V_2) with a top layer depth of 35 cm (a), and 20 cm (b) as well as the depth-extrapolated soil moisture time series based on the uncalibrated modified SMAR (estimated water loss) model presented in this study (top layer depth of 35 cm (c) and 20 cm (d)) based on the CRNS-derived surface soil moisture time series from the standard transfer function and the UTS.

Daily depth-extrapolated soil moisture time series for a depth of 450 cm using the calibrated standard SMAR model (calibrated water loss V_2) with a top layer depth of 35 cm (a), and 20 cm (b) as well as the depth-extrapolated soil moisture time series based on the uncalibrated modified SMAR (estimated water loss) model presented in this study (top layer depth of 35 cm (c) and 20 cm (d)) based on the CRNS-derived surface soil moisture time series from the standard transfer function and the UTS.

Hourly depth-extrapolated soil moisture time series for a depth of 450 cm using the standard SMAR model with a top layer depth of 35 cm (a), and 20 cm (b) as well as the depth-extrapolated soil moisture time series based on the modified SMAR model presented in this study (top layer depth of 35 cm (c) and 20 cm (d)) based on the CRNS-derived surface soil moisture time series from the standard transfer function and the UTS. The soil physical parameters n_1 , n_2 , sc_1 , sc_2 , sw_2 and R_f were optimized by reducing the RMSE against reference soil moisture values in the year 2017. For the original SMAR model, the water loss term V_2 was calibrated instead of R_f .

Daily depth-extrapolated soil moisture time series for a depth of 450 cm using the standard SMAR model with a top layer depth of 35 cm (a), and 20 cm (b) as well as the depth-extrapolated soil moisture time series based on the modified SMAR model presented in this study (top layer depth of 35 cm (c) and 20 cm (d)) based on the CRNS-derived surface soil moisture time series from the standard transfer function and the UTS. The soil physical parameters n_1 , n_2 , sc_1 , sc_2 , sw_2 and R_f were optimized by reducing the RMSE against reference soil moisture values in the year 2017. For the original SMAR model, the water loss term V_2 was calibrated instead of R_f .

Table A2. Statistical goodness-of-fit between the depth-extrapolated *hourly daily* surface soil moisture time series ~~from CRNS~~ and the *average reference* soil moisture time series in the second layer ~~calculated~~ extending from *20 to 200 cm and 300 cm* for the *available in-situ point-scale soil moisture sensors with different scenarios*. Asterisk indicates reaching the *fully-calibrated SMAR and effective parameters in a non-physically-based maximum allowed characteristic time length T value range*. The calibrated model parameters and goodness-of-fit indicators for *during calibration of the original and modified SMAR model are shown* exponential filter method.

Layer 2 extent [cm]	Scenario	Extrapolation approach	Calibration	V ₂ [mm d ⁻¹]	T [d]	RMSE [cm ³ cm ⁻³]	KGE [-]	NSE [-]
20-200	Profile 1	SMAR	Yes	56	-	0.048	-0.175	-15.889
		SMAR _{modified}	No	-	-	0.028	-0.549	-4.836
		exp. Filter	Yes	-	300*	0.031	0.031	-6.158
	Profile 2	SMAR	Yes	8	-	0.059	-0.327	-9.794
		SMAR _{modified}	No	-	-	0.068	-0.469	-13.265
		exp. Filter	Yes	-	1	0.058	0.303	-9.356
	SMN _{arithmetic}	SMAR	Yes	16	-	0.036	0.156	-5.494
		SMAR _{modified}	No	-	-	0.034	-0.242	-4.678
		exp. Filter	Yes	-	23	0.018	0.556	-0.611
	SMN _{weighted}	SMAR	Yes	17	-	0.035	0.133	-5.133
		SMAR _{modified}	No	-	-	0.031	-0.193	-3.907
		exp. Filter	Yes	-	35	0.16	0.606	-0.325
	CRNS _{Revised standard}	SMAR	Yes	51	-	0.032	0.089	-4.089
		SMAR _{modified}	No	-	-	0.027	-0.461	-2.567
		exp. Filter	Yes	-	300*	0.017	0.311	-0.449
	CRNS _{UTS}	SMAR	Yes	47	-	0.32	0.092	-4.128
		SMAR _{modified}	No	-	-	0.026	-0.369	-2.321
		exp. Filter	Yes	-	208	0.016	0.400	-0.255
20-300	Profile 1	SMAR	Yes	81	-	0.032	-0.045	-12.728
		SMAR _{modified}	No	-	-	0.026	-1.150	-8.273
		exp. Filter	Yes	-	300*	0.017	-0.028	-2.987
	Profile 2	SMAR	Yes	21	-	0.044	-0.235	-8.774
		SMAR _{modified}	No	-	-	0.054	-0.492	-14.104
		exp. Filter	Yes	-	1	0.043	-0.298	-8.472
	SMN _{arithmetic}	SMAR	Yes	21	-	0.026	0.232	-4.356
		SMAR _{modified}	No	-	-	0.028	-0.521	-5.113
		exp. Filter	Yes	-	78	0.011	0.581	0.108
	SMN _{weighted}	SMAR	Yes	23	-	0.025	0.249	-4.022
		SMAR _{modified}	No	-	-	0.027	-0.498	-4.576
		exp. Filter	Yes	-	82	0.010	0.596	0.203
	CRNS _{Revised standard}	SMAR	Yes	67	-	0.023	0.184	-3.158
		SMAR _{modified}	No	-	-	0.027	-0.870	-4.717
		exp. Filter	Yes	-	225	0.016	0.302	-1.070
	CRNS _{UTS}	SMAR	Yes	62	-	0.023	0.191	-3.179
		SMAR _{modified}	No	-	-	0.027	-0.769	-4.490
		exp. Filter	Yes	-	182	0.016	0.368	-0.988

Table A3. Statistical goodness-of-fit between the depth-extrapolated *daily* surface soil moisture time from CRNS series and the average reference soil moisture time series in the second layer *calculated-extending* from 20 to 450 cm for the available in-situ point-scale soil moisture sensors with different scenarios. Asterisk indicates reaching the fully-calibrated SMAR and effective parameters in a non-physically-based maximum allowed characteristic time length T value range. The calibrated model parameters and goodness-of-fit indicators for during calibration of the original and modified SMAR model are shown exponential filter method.

Layer 2 extent [cm]	Scenario	Extrapolation approach	Calibration	V_2 [mm d ⁻¹]	T [d]	RMSE [cm ³ cm ⁻³]	KGE [-]	NSE [-]
20-450	Profile 1	SMAR	Yes	181	-	0.013	0.346	-4.083
		SMAR _{modified}	No	-	-	0.031	-2.101	-26.355
		exp. Filter	Yes	-	300*	0.018	-0.508	-7.850
	Profile 2	SMAR	Yes	27	-	0.033	-0.173	-4.179
		SMAR _{modified}	No	-	-	0.044	-0.258	-8.314
		exp. Filter	Yes	-	45	0.032	0.369	-3.916
	SMN _{arithmetic}	SMAR	Yes	38	-	0.015	0.382	-1.65
		SMAR _{modified}	No	-	-	0.023	-0.704	-5.442
		exp. Filter	Yes	-	160	0.015	0.444	-1.728
	SMN _{weighted}	SMAR	Yes	40	-	0.014	0.429	-1.461
		SMAR _{modified}	No	-	-	0.024	-0.827	-6.041
		exp. Filter	Yes	-	152	0.016	0.447	-2.307
	CRNS _{Revised standard}	SMAR	Yes	122	-	0.014	0.427	-1.187
		SMAR _{modified}	No	-	-	0.032	-1.373	-11.435
		exp. Filter	Yes	-	199	0.025	-0.064	-6.573
	CRNS _{UTS}	SMAR	Yes	112	-	0.014	0.427	-1.191
		SMAR _{modified}	No	-	-	0.032	-1.268	-11.385
		exp. Filter	Yes	-	174	0.026	0.022	-6.900

Hourly depth-extrapolated soil moisture time series for a depth of 130 cm using the standard SMAR model with a top layer depth of 35 cm (a), and 20 cm (b) as well as the depth-extrapolated soil moisture time series based on the modified SMAR model presented in this study (top layer depth of 35 cm (c) and 20 cm (d)) based on the CRNS-derived surface soil moisture time series from the standard transfer function and the UTS. The soil physical parameters n_1 , n_2 , sc_1 , sc_2 , sw_2 and R_T were optimized by reducing the RMSE against reference soil moisture values in the year 2017. Here, the parameters sc_1 , sc_2 and sw_2 were calibrated as effective parameters in a non-physically based value range. For the original SMAR model, the water loss term V_2 was calibrated instead of R_T .

Daily depth-extrapolated soil moisture time series for a depth of 130 cm using the standard SMAR model with a top layer depth of 35 cm (a), and 20 cm (b) as well as the depth-extrapolated soil moisture time series based on the modified SMAR model presented in this study (top layer depth of 35 cm (c) and 20 cm (d)) based on the CRNS-derived surface soil moisture time series from the standard transfer function and the UTS. The soil physical parameters n_1 , n_2 , sc_1 , sc_2 , sw_2 and R_T were optimized by reducing the RMSE against reference soil moisture values in the year 2017. Here, the parameters sc_1 , sc_2 and sw_2 were calibrated as effective parameters in a non-physically based value range. For the original SMAR model, the water loss term V_2 was calibrated instead of R_T .

Hourly depth-extrapolated soil moisture time series for a depth of 450 cm using the standard SMAR model with a top layer depth of 35 cm (a), and 20 cm (b) as well as the depth-extrapolated soil moisture time series based on the modified SMAR model presented in this study (top layer depth of 35 cm (c) and 20 cm (d)) based on the CRNS-derived surface soil moisture time series from the standard transfer function and the UTS. The soil physical parameters n_1 , n_2 , sc_1 , sc_2 , sw_2 and R_T were optimized by reducing the RMSE against reference soil moisture values in the year 2017. Here, the parameters sc_1 , sc_2 and sw_2 were calibrated as effective parameters in a non-physically based value range. For the original SMAR model, the water loss term V_2 was calibrated instead of R_T .

Daily depth-extrapolated soil moisture time series for a depth of 450 cm using the standard SMAR model with a top layer depth of 35 cm (a), and 20 cm (b) as well as the depth-extrapolated soil moisture time series based on the modified SMAR model presented in this study (top layer depth of 35 cm (c) and 20 cm (d)) based on the CRNS-derived surface soil moisture time series from the standard transfer function and the UTS. The soil physical parameters n_1 , n_2 , sc_1 , sc_2 , sw_2 and R_T were optimized by reducing the RMSE against reference soil moisture values in the year 2017. Here, the parameters sc_1 , sc_2 and sw_2 were calibrated as effective parameters in a non-physically based value range. For the original SMAR model, the water loss term V_2 was calibrated instead of R_T .

Author contributions. DR further developed the original ideas of TB and AG for this study, performed the data analysis and wrote the manuscript. TB and AG designed the soil moisture monitoring network and contributed to the writing of the manuscript.

Competing interests. The authors declare no competing interests.

Acknowledgements. This study was conducted as part of the research unit Cosmic Sense funded by the German Research Foundation (Deutsche Forschungsgemeinschaft, DFG-FOR2694, project no. 357874777). We gratefully acknowledge the technical support of Markus Morgner, Jörg Wummel and Stephan Schröder who maintain the observation sites in ~~TERENO-NE~~ [TERENO-NorthEast](#) funded by the Helmholtz Association. In addition, we would like to thank Paul Voit for his assistance in data acquisition, field and laboratory work. Further, we would like to thank the Müritz National Park for the continuing support and collaboration. Lastly, we acknowledge the NMDB database (www.nmdb.eu) founded under the European Union's FP7 programme (contract no. 213007), and the PIs of individual neutron monitors for providing data.

765 **References**

- Alaoui, A., Caduff, U., Gerke, H., and Weingartner, R.: Preferential Flow Effects on Infiltration and Runoff in Grassland and Forest Soils, *Vadose Zone Journal*, 10, 367–377, <https://doi.org/10.2136/vzj2010.0076>, 2011.
- Albergel, C., Rüdiger, C., Pellarin, T., Calvet, J.-C., Fritz, N., Froissard, F., Suquia, D., Petitpa, A., Pignatelli, B., and Martin, E.: From near-surface to root-zone soil moisture using an exponential filter: an assessment of the method based on in-situ observations and model
770 simulations, *Hydrology and Earth System Sciences*, 12, 1323–1337, <https://doi.org/10.5194/hess-12-1323-2008>, 2008.
- Altdorff, D., Oswald, S. E., Zacharias, S., Zengerle, C., Dietrich, P., Mollenhauer, H., Attinger, S., and Schrön, M.: Toward Large-Scale Soil Moisture Monitoring Using Rail-Based Cosmic Ray Neutron Sensing, *Water Resources Research*, 59, <https://doi.org/10.1029/2022wr033514>, 2023.
- Andreasen, M., Jensen, K. H., Desilets, D., Franz, T. E., Zreda, M., Bogaen, H. R., and Looms, M. C.: Status and Perspectives on the
775 Cosmic-Ray Neutron Method for Soil Moisture Estimation and Other Environmental Science Applications, *Vadose Zone Journal*, 16, vzj2017.04.0086, <https://doi.org/10.2136/vzj2017.04.0086>, 2017.
- Baatz, R., Bogaen, H. R., Franssen, H.-J. H., Huisman, J. A., Montzka, C., and Vereecken, H.: An empirical vegetation correction for soil water content quantification using cosmic ray probes, *Water Resources Research*, 51, 2030–2046, <https://doi.org/10.1002/2014wr016443>, 2015.
- 780 Babaeian, E., Sadeghi, M., Jones, S. B., Montzka, C., Vereecken, H., and Tuller, M.: Ground, Proximal, and Satellite Remote Sensing of Soil Moisture, *Reviews of Geophysics*, 57, 530–616, <https://doi.org/10.1029/2018rg000618>, 2019.
- Baldwin, D., Manfreda, S., Keller, K., and Smithwick, E.: Predicting root zone soil moisture with soil properties and satellite near-surface moisture data across the conterminous United States, *Journal of Hydrology*, 546, 393–404, <https://doi.org/10.1016/j.jhydrol.2017.01.020>, 2017.
- 785 Baldwin, D., Manfreda, S., Lin, H., and Smithwick, E. A.: Estimating Root Zone Soil Moisture Across the Eastern United States with Passive Microwave Satellite Data and a Simple Hydrologic Model, *Remote Sensing*, 11, 2013, <https://doi.org/10.3390/rs11172013>, 2019.
- Baroni, G. and Oswald, S.: A scaling approach for the assessment of biomass changes and rainfall interception using cosmic-ray neutron sensing, *Journal of Hydrology*, 525, 264–276, <https://doi.org/10.1016/j.jhydrol.2015.03.053>, 2015.
- BKG - German Federal Agency for Cartography and Geodesy: Digital landcover model: ATKIS-Basis-DLM (© GeoBasis-DE/BKG 2018),
790 https://www.bkg.bund.de/SharedDocs/Produktinformationen/BKG/DE/P-2019/191011_ATKISDLM.html, 2018.
- Bogaen, H., Montzka, C., Huisman, J., Graf, A., Schmidt, M., Stockinger, M., von Hebel, C., Hendricks-Franssen, H., van der Kruk, J., Tappe, W., Lücke, A., Baatz, R., Bol, R., Groh, J., Pütz, T., Jakobi, J., Kunkel, R., Sorg, J., and Vereecken, H.: The TERENO-Rur Hydrological Observatory: A Multiscale Multi-Compartment Research Platform for the Advancement of Hydrological Science, *Vadose Zone Journal*, 17, 180055, <https://doi.org/10.2136/vzj2018.03.0055>, 2018.
- 795 Bogaen, H. R., Schrön, M., Jakobi, J., Ney, P., Zacharias, S., Andreasen, M., Baatz, R., Boorman, D., Duygu, M. B., Eguibar-Galán, M. A., Fersch, B., Franke, T., Geris, J., Sanchis, M. G., Kerr, Y., Korf, T., Mengistu, Z., Mialon, A., Nasta, P., Nitychoruk, J., Pinaras, V., Rasche, D., Rosolem, R., Said, H., Schattan, P., Zreda, M., Achleitner, S., Albentosa-Hernández, E., Akyürek, Z., Blume, T., del Campo, A., Canone, D., Dimitrova-Petrova, K., Evans, J. G., Ferraris, S., Frances, F., Gisolo, D., Güntner, A., Herrmann, F., Iwema, J., Jensen, K. H., Kunstmann, H., Lidón, A., Looms, M. C., Oswald, S., Panagopoulos, A., Patil, A., Power, D., Rebmann, C., Romano, N., Scheiffel, L., Seneviratne, S., Weltin, G., and Vereecken, H.: COSMOS-Europe: a European network of cosmic-ray neutron soil moisture sensors,
800 *Earth System Science Data*, 14, 1125–1151, <https://doi.org/10.5194/essd-14-1125-2022>, 2022.

- Bouaziz, L. J. E., Steele-Dunne, S. C., Schellekens, J., Weerts, A. H., Stam, J., Sprokkereef, E., Winsemius, H. H. C., Savenije, H. H. G., and Hrachowitz, M.: Improved Understanding of the Link Between Catchment-Scale Vegetation Accessible Storage and Satellite-Derived Soil Water Index, *Water Resources Research*, 56, <https://doi.org/10.1029/2019wr026365>, 2020.
- 805 Börner, A.: Neue Beiträge zum Naturraum und zur Landschaftsgeschichte im Teilgebiet Serrahn des Müritz-Nationalparks - Forschung und Monitoring, vol. 4, chap. Geologische Entwicklung des Gebietes um den Großen Fürstenseer See, p. 21–29, Geozon Science Media, Berlin, <https://doi.org/10.3285/g.00012>, 2015.
- Canadell, J., Jackson, R. B., Ehleringer, J. B., Mooney, H. A., Sala, O. E., and Schulze, E.-D.: Maximum rooting depth of vegetation types at the global scale, *Oecologia*, 108, 583–595, <https://doi.org/10.1007/bf00329030>, 1996.
- 810 Chandler, K., Stevens, C., Binley, A., and Keith, A.: Influence of tree species and forest land use on soil hydraulic conductivity and implications for surface runoff generation, *Geoderma*, 310, 120–127, <https://doi.org/10.1016/j.geoderma.2017.08.011>, 2018.
- Daly, E. and Porporato, A.: A Review of Soil Moisture Dynamics: From Rainfall Infiltration to Ecosystem Response, *Environmental Engineering Science*, 22, 9–24, <https://doi.org/10.1089/ees.2005.22.9>, 2005.
- Desilets, D., Zreda, M., and Ferré, T. P. A.: Nature's neutron probe: Land surface hydrology at an elusive scale with cosmic rays, *Water Resources Research*, 46, <https://doi.org/10.1029/2009wr008726>, 2010.
- 815 Dimitrova-Petrova, K., Geris, J., Wilkinson, E. M., Rosolem, R., Verrot, L., Lilly, A., and Soulsby, C.: Opportunities and challenges in using catchment-scale storage estimates from cosmic ray neutron sensors for rainfall-runoff modelling, *Journal of Hydrology*, p. 124878, <https://doi.org/10.1016/j.jhydrol.2020.124878>, 2020.
- Dorigo, W., Himmelbauer, I., Aberer, D., Schremmer, L., Petrakovic, I., Zappa, L., Preimesberger, W., Xaver, A., Annor, F., Ardö, J., 820 Baldocchi, D., Bitelli, M., Blöschl, G., Bogena, H., Brocca, L., Calvet, J.-C., Camarero, J. J., Capello, G., Choi, M., Cosh, M. C., van de Giesen, N., Hajdu, I., Ikonen, J., Jensen, K. H., Kanniah, K. D., de Kat, I., Kirchengast, G., Kumar Rai, P., Kyrouac, J., Larson, K., Liu, S., Loew, A., Moghaddam, M., Martínez Fernández, J., Mattar Bader, C., Morbidelli, R., Musial, J. P., Osenga, E., Palecki, M. A., Pellarin, T., Petropoulos, G. P., Pfeil, I., Powers, J., Robock, A., Rüdiger, C., Rummel, U., Strobel, M., Su, Z., Sullivan, R., Tagesson, T., Varlagin, A., Vreugdenhil, M., Walker, J., Wen, J., Wenger, F., Wigneron, J. P., Woods, M., Yang, K., Zeng, Y., Zhang, X., Zreda, M., Dietrich, S., 825 Gruber, A., van Oevelen, P., Wagner, W., Scipal, K., Drusch, M., and Sabia, R.: The International Soil Moisture Network: serving Earth system science for over a decade, *Hydrology and Earth System Sciences*, 25, 5749–5804, <https://doi.org/10.5194/hess-25-5749-2021>, 2021.
- Dorman, L. I.: *Cosmic Rays in the Earth's Atmosphere and Underground*, Astrophysics and Space Science Library, Springer Netherlands, 1 edn., <https://doi.org/10.1007/978-1-4020-2113-8>, 2004.
- 830 Duygu, M. B. and Akyürek, Z.: Using Cosmic-Ray Neutron Probes in Validating Satellite Soil Moisture Products and Land Surface Models, *Water*, 11, 1362, <https://doi.org/10.3390/w11071362>, 2019.
- DWD - German Weather Service: Multi-annual temperature observations 1981-2010, ftp://opendata.dwd.de/climate_environment/CDC/observations_germany/climate/multi_annual/mean_81-10/Temperatur_1981-2010_aktStandort.txt, 2020a.
- DWD - German Weather Service: Multi-annual precipitation observations 1981-2010, ftp://opendata.dwd.de/climate_environment/CDC/observations_germany/climate/multi_annual/mean_81-10/Niederschlag_1981-2010_aktStandort.txt, 2020b.
- 835 Famiglietti, J. S., Ryu, D., Berg, A. A., Rodell, M., and Jackson, T. J.: Field observations of soil moisture variability across scales, *Water Resources Research*, 44, <https://doi.org/10.1029/2006wr005804>, 2008.
- Fan, Y., Miguez-Macho, G., Jobbágy, E. G., Jackson, R. B., and Otero-Casal, C.: Hydrologic regulation of plant rooting depth, *Proceedings of the National Academy of Sciences*, 114, 10 572–10 577, <https://doi.org/10.1073/pnas.1712381114>, 2017.

- 840 Faridani, F., Farid, A., Ansari, H., and Manfreda, S.: A modified version of the SMAR model for estimating root-zone soil moisture from time-series of surface soil moisture, *Water SA*, 43, 492, <https://doi.org/10.4314/wsa.v43i3.14>, 2017.
- Farokhi, M., Faridani, F., Lasaponara, R., Ansari, H., and Faridhosseini, A.: Enhanced Estimation of Root Zone Soil Moisture at 1 km Resolution Using SMAR Model and MODIS-Based Downscaled AMSR2 Soil Moisture Data, *Sensors*, 21, 5211, <https://doi.org/10.3390/s21155211>, 2021.
- 845 Fersch, B., Jagdhuber, T., Schrön, M., Völsch, I., and Jäger, M.: Synergies for Soil Moisture Retrieval Across Scales From Airborne Polarimetric SAR, Cosmic Ray Neutron Roving, and an In Situ Sensor Network, *Water Resources Research*, 54, 9364–9383, <https://doi.org/10.1029/2018wr023337>, 2018.
- Franz, T. E., Zreda, M., Rosolem, R., and Ferre, T. P. A.: A universal calibration function for determination of soil moisture with cosmic-ray neutrons, *Hydrology and Earth System Sciences*, 17, 453–460, <https://doi.org/10.5194/hess-17-453-2013>, 2013.
- 850 Franz, T. E., Wahbi, A., Zhang, J., Vreugdenhil, M., Heng, L., Dercon, G., Strauss, P., Brocca, L., and Wagner, W.: Practical Data Products From Cosmic-Ray Neutron Sensing for Hydrological Applications, *Frontiers in Water*, 2, <https://doi.org/10.3389/frwa.2020.00009>, 2020.
- Gao, X., Zhao, X., Brocca, L., Pan, D., and Wu, P.: Testing of observation operators designed to estimate profile soil moisture from surface measurements, *Hydrological Processes*, 33, 575–584, <https://doi.org/10.1002/hyp.13344>, 2018.
- Gheybi, F., Paridad, P., Faridani, F., Farid, A., Pizarro, A., Fiorentino, M., and Manfreda, S.: Soil Moisture Monitoring in Iran by Implement-
- 855 ing Satellite Data into the Root-Zone SMAR Model, *Hydrology*, 6, 44, <https://doi.org/10.3390/hydrology6020044>, 2019.
- Gugerli, R., Salzmann, N., Huss, M., and Desilets, D.: Continuous and autonomous snow water equivalent measurements by a cosmic ray sensor on an alpine glacier, *The Cryosphere*, 13, 3413–3434, <https://doi.org/10.5194/tc-13-3413-2019>, 2019.
- Guo, X., Fang, X., Zhu, Q., Jiang, S., Tian, J., Tian, Q., and Jin, J.: Estimation of Root-Zone Soil Moisture in Semi-Arid Areas Based on Remotely Sensed Data, *Remote Sensing*, 15, 2003, <https://doi.org/10.3390/rs15082003>, 2023.
- 860 Gupta, H. V., Kling, H., Yilmaz, K. K., and Martinez, G. F.: Decomposition of the mean squared error and NSE performance criteria: Implications for improving hydrological modelling, *Journal of Hydrology*, 377, 80–91, <https://doi.org/10.1016/j.jhydrol.2009.08.003>, 2009.
- Heidbüchel, I., Güntner, A., and Blume, T.: Use of cosmic-ray neutron sensors for soil moisture monitoring in forests, *Hydrology and Earth System Sciences*, 20, 1269–1288, <https://doi.org/10.5194/hess-20-1269-2016>, 2016.
- Heinrich, I., Balanzategui, D., Bens, O., Blasch, G., Blume, T., Böttcher, F., Borg, E., Brademann, B., Brauer, A., Conrad, C., Dietze,
- 865 E., Dräger, N., Fiener, P., Gerke, H. H., Güntner, A., Heine, I., Helle, G., Herbrich, M., Harfenmeister, K., Heußner, K.-U., Hohmann, C., Itzerott, S., Jurasinski, G., Kaiser, K., Kappler, C., Koebsch, F., Liebner, S., Lischeid, G., Merz, B., Missling, K. D., Morgner, M., Pinkerneil, S., Plessen, B., Raab, T., Ruhtz, T., Sachs, T., Sommer, M., Spengler, D., Stender, V., Stüve, P., and Wilken, F.: Interdisciplinary Geo-ecological Research across Time Scales in the Northeast German Lowland Observatory (TERENO-NE), *Vadose Zone Journal*, 17, 180116, <https://doi.org/10.2136/vzj2018.06.0116>, 2018.
- 870 Holgate, C., Jeu, R. D., van Dijk, A., Liu, Y., Renzullo, L., Vinodkumar, Dharssi, I., Parinussa, R., Schalie, R. V. D., Gevaert, A., Walker, J., McJannet, D., Cleverly, J., Haverd, V., Trudinger, C., and Briggs, P.: Comparison of remotely sensed and modelled soil moisture data sets across Australia, *Remote Sensing of Environment*, 186, 479–500, <https://doi.org/10.1016/j.rse.2016.09.015>, 2016.
- Iwema, J., Rosolem, R., Rahman, M., Blyth, E., and Wagener, T.: Land surface model performance using cosmic-ray and point-scale soil moisture measurements for calibration, *Hydrology and Earth System Sciences*, 21, 2843–2861, [https://doi.org/10.5194/hess-21-2843-](https://doi.org/10.5194/hess-21-2843-2017)
- 875 2017, 2017.
- Jackson, R. B., Canadell, J., Ehleringer, J. R., Mooney, H. A., Sala, O. E., and Schulze, E. D.: A global analysis of root distributions for terrestrial biomes, *Oecologia*, 108, 389–411, <https://doi.org/10.1007/bf00333714>, 1996.

- Jackson, T. J., Cosh, M. H., Bindlish, R., Starks, P. J., Bosch, D. D., Seyfried, M., Goodrich, D. C., Moran, M. S., and Du, J.: Validation of Advanced Microwave Scanning Radiometer Soil Moisture Products, *IEEE Transactions on Geoscience and Remote Sensing*, 48, 4256–4272, <https://doi.org/10.1109/tgrs.2010.2051035>, 2010.
- 880 Jakobi, J., Huisman, J. A., Vereecken, H., Diekkrüger, B., and Bogaen, H. R.: Cosmic Ray Neutron Sensing for Simultaneous Soil Water Content and Biomass Quantification in Drought Conditions, *Water Resources Research*, 54, 7383–7402, <https://doi.org/10.1029/2018wr022692>, 2018.
- Jost, G., Schume, H., Hager, H., Markart, G., and Kohl, B.: A hillslope scale comparison of tree species influence on soil moisture dynamics and runoff processes during intense rainfall, *Journal of Hydrology*, 420–421, 112–124, <https://doi.org/10.1016/j.jhydrol.2011.11.057>, 2012.
- 885 Kiese, R., Fersch, B., Baessler, C., Brosy, C., Butterbach-Bahl, K., Chwala, C., Dannenmann, M., Fu, J., Gasche, R., Grote, R., Jahn, C., Klatt, J., Kunstmann, H., Mauder, M., Rödiger, T., Smiatek, G., Soltani, M., Steinbrecher, R., Völksch, I., Werhahn, J., Wolf, B., Zeeman, M., and Schmid, H.: The TERENO Pre-Alpine Observatory: Integrating Meteorological, Hydrological, and Biogeochemical Measurements and Modeling, *Vadose Zone Journal*, 17, 180 060, <https://doi.org/10.2136/vzj2018.03.0060>, 2018.
- 890 Kodama, M., Nakai, K., Kawasaki, S., and Wada, M.: An application of cosmic-ray neutron measurements to the determination of the snow-water equivalent, *Journal of Hydrology*, 41, 85–92, [https://doi.org/10.1016/0022-1694\(79\)90107-0](https://doi.org/10.1016/0022-1694(79)90107-0), 1979.
- Kodama, M., Kudo, S., and Kosuge, T.: Application of atmospheric neutrons to soil moisture measurement, *Soil Science*, 140, 237–242, 1985.
- Köhli, M., Schrön, M., Zreda, M., Schmidt, U., Dietrich, P., and Zacharias, S.: Footprint characteristics revised for field-scale soil moisture monitoring with cosmic-ray neutrons, *Water Resources Research*, 51, 5772–5790, <https://doi.org/10.1002/2015wr017169>, 2015.
- 895 Köhli, M., Weimar, J., Schrön, M., Baatz, R., and Schmidt, U.: Soil Moisture and Air Humidity Dependence of the Above-Ground Cosmic-Ray Neutron Intensity, *Frontiers in Water*, 2, <https://doi.org/10.3389/frwa.2020.544847>, 2021.
- LAIV-MV - State Agency for Interior Administration Mecklenburg-Western Pomerania: Digital elevation model: ATKIS-DEMI (© GeoBasis-DE/M-V 2011), <https://www.laiv-mv.de/Geoinformation/Geobasisdaten/Gelaendemodelle/>, 2011.
- 900 Li, D., Schrön, M., Köhli, M., Bogaen, H., Weimar, J., Bello, M. A. J., Han, X., Gimeno, M. A. M., Zacharias, S., Vereecken, H., and Franssen, H.-J. H.: Can Drip Irrigation be Scheduled with Cosmic-Ray Neutron Sensing?, *Vadose Zone Journal*, 18, 190 053, <https://doi.org/10.2136/vzj2019.05.0053>, 2019a.
- Li, J. and Zhang, L.: Comparison of Four Methods for Vertical Extrapolation of Soil Moisture Contents from Surface to Deep Layers in an Alpine Area, *Sustainability*, 13, 8862, <https://doi.org/10.3390/su13168862>, 2021.
- 905 Li, X., Gentile, P., Lin, C., Zhou, S., Sun, Z., Zheng, Y., Liu, J., and Zheng, C.: A simple and objective method to partition evapotranspiration into transpiration and evaporation at eddy-covariance sites, *Agricultural and Forest Meteorology*, 265, 171–182, <https://doi.org/10.1016/j.agrformet.2018.11.017>, 2019b.
- Manfreda, S., Brocca, L., Moramarco, T., Melone, F., and Sheffield, J.: A physically based approach for the estimation of root-zone soil moisture from surface measurements, *Hydrology and Earth System Sciences*, 18, 1199–1212, <https://doi.org/10.5194/hess-18-1199-2014>,
- 910 2014.
- Mares, V., Brall, T., Bütikofer, R., and Rühm, W.: Influence of environmental parameters on secondary cosmic ray neutrons at high-altitude research stations at Jungfrauoch, Switzerland, and Zugspitze, Germany, *Radiation Physics and Chemistry*, 168, 108 557, <https://doi.org/10.1016/j.radphyschem.2019.108557>, 2020.

- 915 Maysonnave, J., Delpierre, N., François, C., Jourdan, M., Cornut, I., Bazot, S., Vincent, G., Morfin, A., and Berveiller, D.: Contribution of deep soil layers to the transpiration of a temperate deciduous forest: Implications for the modelling of productivity, *Science of The Total Environment*, 838, 155–181, <https://doi.org/10.1016/j.scitotenv.2022.155981>, 2022.
- McJannet, D., Hawdon, A., Baker, B., Renzullo, L., and Searle, R.: Multiscale soil moisture estimates using static and roving cosmic-ray soil moisture sensors, *Hydrology and Earth System Sciences*, 21, 6049–6067, <https://doi.org/10.5194/hess-21-6049-2017>, 2017.
- 920 Montzka, C., Bogena, H., Zreda, M., Monerris, A., Morrison, R., Muddu, S., and Vereecken, H.: Validation of Spaceborne and Modelled Surface Soil Moisture Products with Cosmic-Ray Neutron Probes, *Remote Sensing*, 9, 103, <https://doi.org/10.3390/rs9020103>, 2017.
- Neumann, R. B. and Cardon, Z. G.: The magnitude of hydraulic redistribution by plant roots: a review and synthesis of empirical and modeling studies, *New Phytologist*, 194, 337–352, <https://doi.org/10.1111/j.1469-8137.2012.04088.x>, 2012.
- 925 Nguyen, H. H., Jeong, J., and Choi, M.: Extension of cosmic-ray neutron probe measurement depth for improving field scale root-zone soil moisture estimation by coupling with representative in-situ sensors, *Journal of Hydrology*, 571, 679–696, <https://doi.org/10.1016/j.jhydrol.2019.02.018>, 2019.
- Nimmo, J. R.: The processes of preferential flow in the unsaturated zone, *Soil Science Society of America Journal*, 85, 1–27, <https://doi.org/10.1002/saj2.20143>, 2021.
- Patil, A. and Ramsankaran, R.: Improved streamflow simulations by coupling soil moisture analytical relationship in EnKF based hydrological data assimilation framework, *Advances in Water Resources*, 121, 173–188, <https://doi.org/10.1016/j.advwatres.2018.08.010>, 2018.
- 930 Paul-Limoges, E., Wolf, S., Schneider, F. D., Longo, M., Moorcroft, P., Gharun, M., and Damm, A.: Partitioning evapotranspiration with concurrent eddy covariance measurements in a mixed forest, *Agricultural and Forest Meteorology*, 280, 107–116, <https://doi.org/10.1016/j.agrformet.2019.107786>, 2020.
- Peterson, A. M., Helgason, W. D., and Ireson, A. M.: Estimating field-scale root zone soil moisture using the cosmic-ray neutron probe, *Hydrology and Earth System Sciences*, 20, 1373–1385, <https://doi.org/10.5194/hess-20-1373-2016>, 2016.
- 935 Pierret, A., Maeght, J.-L., Clément, C., Montoroi, J.-P., Hartmann, C., and Gonkhamdee, S.: Understanding deep roots and their functions in ecosystems: an advocacy for more unconventional research, *Annals of Botany*, 118, 621–635, <https://doi.org/10.1093/aob/mcw130>, 2016.
- Poggio, L., de Sousa, L. M., Batjes, N. H., Heuvelink, G. B. M., Kempen, B., Ribeiro, E., and Rossiter, D.: SoilGrids 2.0: producing soil information for the globe with quantified spatial uncertainty, *SOIL*, 7, 217–240, <https://doi.org/10.5194/soil-7-217-2021>, 2021.
- R Core Team: R: A Language and Environment for Statistical Computing, R Foundation for Statistical Computing, Vienna, Austria, r version 940 3.5.1 (2018-07-02) edn., <https://www.R-project.org/>, 2018.
- R Core Team: R: A Language and Environment for Statistical Computing, R Foundation for Statistical Computing, Vienna, Austria, r version 4.3.2 (2023-10-31 ucrt) edn., <https://www.R-project.org/>, 2023.
- 945 Rasche, D., Weimar, J., Schrön, M., Köhli, M., Morgner, M., Güntner, A., and Blume, T.: A change in perspective: downhole cosmic-ray neutron sensing for the estimation of soil moisture, *Hydrology and Earth System Sciences*, 27, 3059–3082, <https://doi.org/10.5194/hess-27-3059-2023>, 2023.
- Rosolem, R., Shuttleworth, W. J., Zreda, M., Franz, T. E., Zeng, X., and Kurc, S. A.: The Effect of Atmospheric Water Vapor on Neutron Count in the Cosmic-Ray Soil Moisture Observing System, *Journal of Hydrometeorology*, 14, 1659–1671, <https://doi.org/10.1175/jhm-d-12-0120.1>, 2013.
- 950 Schattan, P., Baroni, G., Oswald, S. E., Schöber, J., Fey, C., Kormann, C., Huttenlau, M., and Achleitner, S.: Continuous monitoring of snowpack dynamics in alpine terrain by aboveground neutron sensing, *Water Resources Research*, 53, 3615–3634, <https://doi.org/10.1002/2016wr020234>, 2017.

- Schattan, P., Köhli, M., Schrön, M., Baroni, G., and Oswald, S. E.: Sensing Area-Average Snow Water Equivalent with Cosmic-Ray Neutrons: The Influence of Fractional Snow Cover, *Water Resources Research*, 55, 10796–10812, <https://doi.org/10.1029/2019wr025647>, 2019.
- 955 Schrön, M., Köhli, M., Scheffele, L., Iwema, J., Bogena, H. R., Lv, L., Martini, E., Baroni, G., Rosolem, R., Weimar, J., Mai, J., Cuntz, M., Rebmann, C., Oswald, S. E., Dietrich, P., Schmidt, U., and Zacharias, S.: Improving calibration and validation of cosmic-ray neutron sensors in the light of spatial sensitivity, *Hydrology and Earth System Sciences*, 21, 5009–5030, <https://doi.org/10.5194/hess-21-5009-2017>, 2017.
- Schrön, M., Rosolem, R., Köhli, M., Piussi, L., Schröter, I., Iwema, J., Kögler, S., Oswald, S. E., Wollschläger, U., Samaniego, L., Dietrich, P., and Zacharias, S.: Cosmic-ray Neutron Rover Surveys of Field Soil Moisture and the Influence of Roads, *Water Resources Research*, 960 54, 6441–6459, <https://doi.org/10.1029/2017wr021719>, 2018a.
- Schrön, M., Zacharias, S., Womack, G., Köhli, M., Desilets, D., Oswald, S. E., Bumberger, J., Mollenhauer, H., Kögler, S., Remmler, P., Kasner, M., Denk, A., and Dietrich, P.: Intercomparison of cosmic-ray neutron sensors and water balance monitoring in an urban environment, *Geoscientific Instrumentation, Methods and Data Systems*, 7, 83–99, <https://doi.org/10.5194/gi-7-83-2018>, 2018b.
- Schrön, M., Oswald, S. E., Zacharias, S., Kasner, M., Dietrich, P., and Attinger, S.: Neutrons on Rails: Transregional Monitoring of Soil 965 Moisture and Snow Water Equivalent, *Geophysical Research Letters*, 48, <https://doi.org/10.1029/2021gl093924>, 2021.
- Schume, H., Jost, G., and Katzensteiner, K.: Spatio-temporal analysis of the soil water content in a mixed Norway spruce (*Picea abies* (L.) Karst.)–European beech (*Fagus sylvatica* L.) stand, *Geoderma*, 112, 273–287, [https://doi.org/10.1016/s0016-7061\(02\)00311-7](https://doi.org/10.1016/s0016-7061(02)00311-7), 2003.
- Seneviratne, S. I., Corti, T., Davin, E. L., Hirschi, M., Jaeger, E. B., Lehner, I., Orlowsky, B., and Teuling, A. J.: Investigating soil moisture–climate interactions in a changing climate: A review, *Earth-Science Reviews*, 99, 125–161, 970 <https://doi.org/10.1016/j.earscirev.2010.02.004>, 2010.
- Sponagel, H., Grottenthaler, W., Hartmann, K.-J., Hartwich, R., Janetzko, P., Joisten, H., Kühn, D., Sabel, K.-J., and Traidl, R.: *Bodenkundliche Kartieranleitung KA5*, BGR - German Federal Institute for Geosciences and Natural Resources, Hannover, Germany, 5 edn., 2005.
- Stevanato, L., Baroni, G., Cohen, Y., Lino, F. C., Gatto, S., Lunardon, M., Marinello, F., Moretto, S., and Morselli, L.: A Novel Cosmic-Ray 975 Neutron Sensor for Soil Moisture Estimation over Large Areas, *Agriculture*, 9, 202, <https://doi.org/10.3390/agriculture9090202>, 2019.
- Tian, J., Han, Z., Bogena, H. R., Huisman, J. A., Montzka, C., Zhang, B., and He, C.: Estimation of subsurface soil moisture from surface soil moisture in cold mountainous areas, *Hydrology and Earth System Sciences*, 24, 4659–4674, <https://doi.org/10.5194/hess-24-4659-2020>, 2020.
- Tian, Z., Li, Z., Liu, G., Li, B., and Ren, T.: Soil water content determination with cosmic-ray neutron sensor: Correcting aboveground 980 hydrogen effects with thermal/fast neutron ratio, *Journal of Hydrology*, 540, 923–933, <https://doi.org/10.1016/j.jhydrol.2016.07.004>, 2016.
- Vather, T., Everson, C., and Franz, T. E.: Calibration and Validation of the Cosmic Ray Neutron Rover for Soil Water Mapping within Two South African Land Classes, *Hydrology*, 6, 65, <https://doi.org/10.3390/hydrology6030065>, 2019.
- Vather, T., Everson, C. S., and Franz, T. E.: The Applicability of the Cosmic Ray Neutron Sensor to Simultaneously Monitor Soil Water Content and Biomass in an *Acacia mearnsii* Forest, *Hydrology*, 7, 48, <https://doi.org/10.3390/hydrology7030048>, 2020.
- 985 Vereecken, H., Huisman, J. A., Bogena, H., Vanderborght, J., Vrugt, J. A., and Hopmans, J. W.: On the value of soil moisture measurements in vadose zone hydrology: A review, *Water Resources Research*, 44, <https://doi.org/10.1029/2008wr006829>, 2008.
- Vereecken, H., Huisman, J., Pachepsky, Y., Montzka, C., van der Kruk, J., Bogena, H., Weihermüller, L., Herbst, M., Martinez, G., and Vanderborght, J.: On the spatio-temporal dynamics of soil moisture at the field scale, *Journal of Hydrology*, 516, 76–96, <https://doi.org/10.1016/j.jhydrol.2013.11.061>, 2014.

- 990 Wagner, W., Lemoine, G., and Rott, H.: A Method for Estimating Soil Moisture from ERS Scatterometer and Soil Data, *Remote Sensing of Environment*, 70, 191–207, [https://doi.org/10.1016/s0034-4257\(99\)00036-x](https://doi.org/10.1016/s0034-4257(99)00036-x), 1999.
- Wang, C., Fu, B., Zhang, L., and Xu, Z.: Soil moisture–plant interactions: an ecohydrological review, *Journal of Soils and Sediments*, 19, 1–9, <https://doi.org/10.1007/s11368-018-2167-0>, 2018.
- 995 Wang, T., Franz, T. E., You, J., Shulski, M. D., and Ray, C.: Evaluating controls of soil properties and climatic conditions on the use of an exponential filter for converting near surface to root zone soil moisture contents, *Journal of Hydrology*, 548, 683–696, <https://doi.org/10.1016/j.jhydrol.2017.03.055>, 2017.
- Weimar, J., Köhli, M., Budach, C., and Schmidt, U.: Large-Scale Boron-Lined Neutron Detection Systems as a ^3He Alternative for Cosmic Ray Neutron Sensing, *Frontiers in Water*, 2, 16, <https://doi.org/10.3389/frwa.2020.00016>, 2020.
- Zacharias, S., Bogena, H., Samaniego, L., Mauder, M., Fuß, R., Pütz, T., Frenzel, M., Schwank, M., Baessler, C., Butterbach-Bahl, K., Bens, O., Borg, E., Brauer, A., Dietrich, P., Hajnsek, I., Helle, G., Kiese, R., Kunstmann, H., Klotz, S., Munch, J. C., Papen, H., Priesack, E., Schmid, H. P., Steinbrecher, R., Rosenbaum, U., Teutsch, G., and Vereecken, H.: A Network of Terrestrial Environmental Observatories in Germany, *Vadose Zone Journal*, 10, 955–973, <https://doi.org/10.2136/vzj2010.0139>, 2011.
- 1000 Zambrano-Bigiarini, M.: hydroGOF: Goodness-of-fit functions for comparison of simulated and observed hydrological time series, <https://doi.org/https://zenodo.org/records/840087>, r package version 0.3-10, 2017.
- 1005 Zambrano-Bigiarini, M.: hydroGOF: Goodness-of-fit functions for comparison of simulated and observed hydrological time series, <https://doi.org/https://zenodo.org/records/3707013>, r package version 0.4-0, 2020.
- Zhang, N., Quiring, S., Ochsner, T., and Ford, T.: Comparison of Three Methods for Vertical Extrapolation of Soil Moisture in Oklahoma, *Vadose Zone Journal*, 16, [vzj2017.04.0085](https://doi.org/10.2136/vzj2017.04.0085), <https://doi.org/10.2136/vzj2017.04.0085>, 2017.
- Zhu, X., Shao, M., Jia, X., Huang, L., Zhu, J., and Zhang, Y.: Application of temporal stability analysis in depth-scaling estimated soil water content by cosmic-ray neutron probe on the northern Tibetan Plateau, *Journal of Hydrology*, 546, 299–308, <https://doi.org/10.1016/j.jhydrol.2017.01.019>, 2017.
- 1010 Zhuang, R., Zeng, Y., Manfreda, S., and Su, Z.: Quantifying Long-Term Land Surface and Root Zone Soil Moisture over Tibetan Plateau, *Remote Sensing*, 12, 509, <https://doi.org/10.3390/rs12030509>, 2020.
- Zreda, M., Desilets, D., Ferré, T. P. A., and Scott, R. L.: Measuring soil moisture content non-invasively at intermediate spatial scale using cosmic-ray neutrons, *Geophysical Research Letters*, 35, <https://doi.org/10.1029/2008gl035655>, 2008.
- 1015 Zreda, M., Shuttleworth, W. J., Zeng, X., Zweck, C., Desilets, D., Franz, T., and Rosolem, R.: COSMOS: the COsmic-ray Soil Moisture Observing System, *Hydrology and Earth System Sciences*, 16, 4079–4099, <https://doi.org/10.5194/hess-16-4079-2012>, 2012.